

A Portable Framework for Accelerating Stencil Computations on Modern Node Architectures

RYUICHI SAI, Rice University, USA

JOHN MELLOR-CRUMMEY, Rice University, USA

JINFAN XU, Rice University, USA

MAURICIO ARAYA-POLO, TotalEnergies EP Research & Technology US, LLC., USA

Finite-difference methods based on high-order stencils are widely used in seismic simulations, weather forecasting, computational fluid dynamics, and other scientific applications. Achieving HPC-level stencil computations on one architecture is challenging, porting to other architectures without sacrificing performance requires significant effort, especially in this golden age of many distinctive architectures.

To help developers achieve performance, portability, and productivity with stencil computations, we developed StencilPy. With StencilPy, developers write stencil computations in a high-level domain-specific language, which promotes productivity, while its backends generate efficient code for existing and emerging architectures, including modern many-core CPUs (such as AMD Genoa-X, Fujitsu A64FX, and Intel Sapphire Rapids), latest generations of GPUs (including NVIDIA H100 and A100, AMD MI200, and Intel Ponte Vecchio), and accelerators (including Cerebras and STX). StencilPy demonstrates promising performance results on par with hand-written code, maintains cross-architectural performance portability, and enhances productivity. Its modular design enables easy configuration, customization, and extension.

A 25-point star-shaped stencil written in StencilPy is one-quarter of the length of a hand-crafted CUDA code and achieves similar performance on an NVIDIA H100 GPU. In addition, the same kernel written using our tool is 7× shorter than hand-optimized code written in Cerebras Software Language (CSL), and it delivers comparable performance that code on a Cerebras CS-2.

CCS Concepts: • **Software and its engineering** → **Domain specific languages; Source code generation**; • **General and reference** → **Performance**; • **Computing methodologies** → **Massively parallel and high-performance simulations**.

Additional Key Words and Phrases: Domain specific language, automated code generation, high-order stencil computations, high-performance computing, GPU, Cerebras, emerging architectures.

1 INTRODUCTION

With the diversity of architectures available to application developers, achieving performance, portability, and productivity (3Ps) has become increasingly important. Adopting a 3Ps approach can simplify the development and maintenance of scientific applications, enabling them to run efficiently on multiple architectures without sacrificing performance.

However, achieving this goal has always been challenging due to the inherent trade-offs among performance, portability, and productivity. Achieving high performance and portability requires implementing algorithms that exploit low-level hardware features. On the other hand, productivity is accomplished with higher-level software abstractions that hide these low-level details. The problem becomes more significant with modern node architectures, as low-level hardware details vary between architectures, vendors, and even different generations of products from the same vendor. Additionally, hardware vendors lack unified programming models, and occasionally, even the programming models and frameworks provided by the same vendor change significantly over time. As a result, developing, optimizing,

Authors' addresses: Ryuichi Sai, ryuichi@rice.edu, Rice University, 6100 Main Street, MS-132, Houston, Texas, USA, 77005; John Mellor-Crummey, Rice University, 6100 Main Street, MS-132, Houston, Texas, USA, 77005; Jinfan Xu, Rice University, 6100 Main Street, MS-132, Houston, Texas, USA, 77005; Mauricio Araya-Polo, TotalEnergies EP Research & Technology US, LLC., Houston, Texas, USA.

and maintaining scientific applications is costly due to the diversity of architectures, programming models, and the evolution of vendor software stacks.

Stencil computation is widely used in many scientific applications, such as modeling of seismic wave propagation, weather forecasting, computational fluid dynamics, and convolutional neural networks. Therefore, achieving 3Ps for stencil computations is of great interest. While a 25-point star-shaped stencil update from a global view requires only ten lines of C code, our highly optimized GPU kernel for the same stencil computation required 375 lines of CUDA code and more than 600 lines of auxiliary code in C [57, 59]. Furthermore, manually porting a similar stencil code to a Cerebras CS-2 system (CS2) needed 1613 lines of CSL code and 364 lines of Python code [9]. Accelerating such kernels on these platforms requires complex algorithms, optimization strategies, careful data allocations, and handling intricate data movement. Therefore, they are also difficult to program and unable to port between systems.

A portable framework for accelerating stencil computations is needed to address these challenges and achieve 3Ps for high-order stencil computations on modern node architectures. To address this need, we have been developing StencilPy—a portable Python framework for implementing stencil computations. The framework’s frontend enables developers to express common stencil computations using a high-level abstraction with a global-view logic, thus maintaining high developer productivity. Its platform-agnostic syntax and kernel launch invocation facilitate porting to various systems without changing the implementation. The backend generates high-performance executables for modern node architectures, including modern GPUs and several accelerators. The framework also explores ways to reduce overhead during code analysis and generation while providing a user-friendly interface for domain experts to specify optimizations and facilitate evaluations.

This manuscript presents our progress on StencilPy, a portable framework for accelerating stencil computations on modern node architectures, including a Python-hosted domain-specific language and code generators for modern many-core CPUs (such as AMD Genoa-X, Fujitsu A64FX [19], and Intel Sapphire Rapids), latest generations of GPUs (including NVIDIA H100 and A100, AMD MI200, and Intel Ponte Vecchio), and accelerators (including Cerebras [8] and STX [14]). While our goal is to support stencils of commonly used shapes and different orders, our effort to date has focused primarily on high-order stencils. In this chapter, we evaluate our framework using a 25-point star-shaped stencil commonly used by the energy industry for the acoustic isotropic approximation of the wave equation as part of seismic imaging [41]. This manuscript describes the following contributions:

- the design of an embedded domain-specific language (DSL) for expressing stencil computations in Python;
- the implementation of a framework that parses and analyzes the DSL, generates platform-specific code for modern CPUs (AMD Genoa-X, Apple Silicon, Fujitsu A64FX, IBM Power, and Intel Sapphire Rapids), multiple generations of GPUs of different vendors (NVIDIA H100, A100, and V100; AMD MI200 and MI100; and Intel Ponte Vecchio), and accelerators (STX [14] and Cerebras CS-2 [8]);
- optimization strategies that minimize overheads associated with the StencilPy framework and accelerate runtime performance; and
- a performance evaluation based on a 25-point star-shaped high-order stencil used for seismic imaging.

The next section provides some background about stencil computations. Section 3 reviews related work. Section 4 describes the framework’s design and architecture. Section 5 introduces the DSL and frontend. Section 6 describes the implementation of the StencilPy framework. Section 7 provides an overview of StencilPy’s optimizations to boost stencil runtime performance. Sections 8 and 9 describe the framework’s workflow and its backend templates, respectively. Section 10 describes StencilPy’s intermediate representations. Section 11 extensively describes code

generation. Section 12 explores options to customize and extend the framework beyond its current capabilities. Section 13 describes our evaluation methodologies to assess numerical correctness, performance, portability, and productivity, and then it reviews our findings. Sections 14 and 15 summarize our conclusions and discuss future work.

2 BACKGROUND

To help the reader understand the domain applications StencilPy targets, we provide a brief introduction to high-order stencil computations, especially ones used in seismic modeling.

2.1 High-Order Stencil Computations

In stencil computations, data elements from a multi-dimensional array are iteratively updated according to a fixed pattern. In this work, an array is manipulated as a Cartesian grid. An element in the grid is usually called a cell or a point. Calculating the next value for a cell using a stencil involves computing a weighted sum of products between values of a set of neighboring cells (stencil defines the set of cells used) and scaling coefficients.

Applying a stencil pattern to the points in a block requires values for points in neighboring blocks. The points needed from neighboring blocks are collectively known as the halo region. The thickness of the halo along each dimension is called the halo size or halo width, and it also defines the order of the stencil. When a stencil has a large halo width, it is called a high-order stencil. Stencil computations are applied to all the elements of a grid over a sequence of iterations, until the underlying equation converges.

2.2 Seismic Modeling and Acoustic Isotropic Approximation

In this manuscript, we study high-order stencil-based implementations of the acoustic isotropic approximation (Acoustic ISO) of the wave equation [41], which is commonly used by the energy industry on large grids to model and characterize the subsurface for a variety of purposes.

The wave equation for an acoustic isotropic operator with constant-density has the following form:

$$\frac{1}{V^2} \frac{\partial^2 \mathbf{u}}{\partial t^2} - \nabla^2 \mathbf{u} = \mathbf{f}, \quad (1)$$

where $\mathbf{u} = \mathbf{u}(x, y, z)$ is the wavefield, V is the Earth model (with velocity as rock property), and \mathbf{f} is the source perturbation. The equation is discretized in time using a second-order centered stencil, resulting in the semi-discretized equation:

$$\mathbf{u}^{n+1} - \mathbf{Q}\mathbf{u}^n + \mathbf{u}^{n-1} = \left(\Delta t^2\right) \mathbf{V}^2 \mathbf{f}^n, \text{ with } \mathbf{Q} = 2 + \Delta t^2 \mathbf{V}^2 \nabla^2. \quad (2)$$

Finally, the equation is discretized in space using a 25-point stencil in 3D, with eight points in along each axis surrounding a center point, where c_{xyz} , c_{xm} , c_{ym} , c_{zm} are the discretization parameters:

Input:
 f: source

Output:
 \mathbf{u}^n : wavefield at timestep n , for $n \leftarrow 1$ to T

$\mathbf{u}^0 := 0$;

for $n \leftarrow 1$ to T **do**

for each point in wavefield \mathbf{u}^n **do**

Solve Eq. 2 (left hand side) for wavefield \mathbf{u}^n ;

end

$\mathbf{u}^n = \mathbf{u}^n + \mathbf{f}^n$ (Eq. 2 right hand side);

end

Algorithm 1: A high-level description of the algorithm for solving the acoustic isotropic approximation of the wave equation with constant density.

$$\begin{aligned} \nabla^2 \mathbf{u}(x, y, z) \approx & c_{xyz} \times \mathbf{u}(i, j, k) + \\ & \sum_{m=1}^4 (c_{xm} \times [\mathbf{u}(i+m, j, k) + \mathbf{u}(i-m, j, k)] + \\ & c_{ym} \times [\mathbf{u}(i, j+m, k) + \mathbf{u}(i, j-m, k)] + \\ & c_{zm} \times [\mathbf{u}(i, j, k+m) + \mathbf{u}(i, j, k-m)]) \end{aligned} \quad (3)$$

A high-level description of the algorithm is shown in Algorithm 1. As is common for seismic modeling, the simulations employ a Perfectly-Matched Layer (PML) [30] boundary condition around the simulation domain. The resulting extended domain consists of an “inner” region and a surrounding “PML” region. As described later in this manuscript, our framework is designed to decompose the data domain and launch dedicated kernels accordingly to achieve great performance.

This kernel involves applying a star-shaped 25-point stencil, as depicted in Figure 1, to elements of a 3D array. Computation in the PML region is more complex than that in the inner region. The PML region employs the same 25-point stencil applied in the inner region and also a 7-point star-shaped stencil to a different array to compute boundary conditions.

The grid, representing the physical domain, tends to be substantial in production simulations. Each of its dimensions is usually large with up to thousands of points. To simulate how the waves propagate through the domain, it is necessary to apply the stencil computations iteratively for a large number of time steps.

3 RELATED WORK

There is much prior work [12, 13, 15–17, 21, 25, 29, 31, 39, 40, 42, 44, 48, 50, 60, 62–65] exploring accelerating stencil computations using a compiler-assist approach. Here, we describe the ones most relevant to our work.

Stencil Optimizations. Time skewing [29, 40, 60, 64, 65] avoids costly data movement by skewing data dimension(s) by the time dimension so that cached data is reused for multiple time steps. Cache-oblivious algorithms [15–17, 62, 63] tile the domain and performs a space cut or a time cut to maximize the use of each memory level. Overlapped tiling

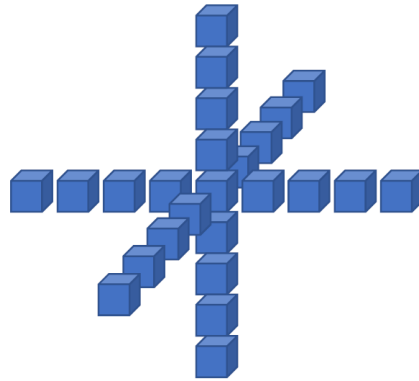


Fig. 1. A star-shaped 25-point stencil.

uses time skewing to trade redundant computation along the boundaries of overlapped tiles for a reduction in memory bandwidth required [25, 31]. Split tiling [21], on the other hand, mitigates redundant computations by employing a two-phase computation approach. In the first phase, hyper-trapezoidal tiles along the time dimension are used, and in the second phase, the missing points are backfilled.

Streaming on the outermost dimension is a widely used optimization technique for accelerating high-order stencils on GPUs [58, 59]. Nguyen et al. [44] introduced a 2.5D spatial blocking technique, which was further extended to a 3.5D blocking algorithm by combining it with 1D temporal blocking. Micikevicius [42] used registers to store data elements along a streaming dimension to improve performance. Matsumura et al. [39] refined this approach by incorporating fixed register allocations, double buffering, and a division of the streaming dimension. In our work, we leverage these optimization techniques for GPU and STX backends in our code generation and optimization process.

The Semi-stencil algorithm [12, 13] is a technique that divides a stencil computation into two parts: a forward update and a backward update. This partitioning offers a tradeoff between the number of loads and stores involved in the computation. In our work, we leverage the Semi-stencil algorithm for certain high-order stencils on both GPU and STX backends. This approach proves advantageous due to the significant reduction in the number of loads required for high-order stencils, resulting in improved performance.

While previous work primarily emphasizes performance and relies on hand-crafted code for evaluation, our work also highlights performance portability and productivity by leveraging the power of compiler technologies.

Stencil DSLs and automated code generations. Domain-Specific Languages (DSLs) for stencil computations have been widely studied [3, 4, 10, 35, 46, 49–51, 63]. Rawat et al. [49] use Directed Acyclic Graphs (DAGs) to analyze register dependencies and optimize the ordering of registers for improved performance. Rawat et al. [51] later enhance this approach by incorporating dynamic resource allocations with automatic tuning techniques. BrickLib [2] leverages fine-grained data blocking and generates vector code for the blocks to achieve great performance portability on CPUs and GPUs. Diamond tiling using a polyhedral model [5, 7] has been studied and integrated into modern compilers and their toolchains. Several prior work [18, 20, 22] propose various reusable designs for multi-layer intermediate representations, aiming to enhance the utilization of these representations between DSL frontends and code generations. STELLA [23] integrates within the standard C++ template meta-programming, and application developers can fall back

on the host language if they need to incorporate features not supported by the library. Halide [46] introduces a DSL embedded in C++ rather than being a standalone language. It builds an in-memory representation using Halide’s C++ API, which can be compiled ahead-of-time or just-in-time.

For distributed memory architectures, such as the ones in dataflow architecture, stencil computation strategies are studied in High Performance Fortran [53, 54].

Functional programming [37, 61] has also been explored in the past for robust reasoning of the stencil computations and their optimizations.

These studies inspire our work, and we also aim for performance portability and developer productivity. Our framework also generates code for a broader range of modern node architectures.

Software Frameworks in Python. We have drawn inspiration from Numpy [24]—a comprehensive Python library for scientific numerical computations. Numpy implements performance-critical components in the C language while keeping the user-facing frontend in Python. We adopt a similar approach, but our specialization is stencil computations rather than general-purpose computations.

Numba [32] delegates machine code optimizations and generations at runtime to LLVM [33]. It leverages the standard Python interpreter while annotating Numba code regions with decorators. Similarly, we use decorators, but our approach involves generating code using platform-specific programming models and employing platform-specific compilers for building the generated code.

Other specialized frameworks, such as Taichi [26], TensorFlow [1], and PyTorch [45], follow a similar architectural design to Numpy. Mojo [43] is a superset of Python that uses LLVM [33] and MLIR [34] for code generation. It uses inferred static typing. However, these frameworks primarily focus on domains such as machine learning, image processing, or artificial intelligence, whereas our framework specializes in stencil computations. While our framework does not support type inference, our code optimization and generation need type information. Therefore, our framework requires type hints for stencil target and kernel functions.

APPy [66] annotates Python code using a syntax similar to that of OpenMP’s pragmas. It focuses on loop-level optimization and automates code vectorization on GPUs. Similarly, our framework offers GPU templates that facilitate vectorization, with a particular focus on Stencil computation.

Frameworks specifically designed for stencils, such as PyStencil [6] and Devito [35, 36], offer domain application developers the ability to express their applications at high levels of abstraction, such as in the domains of physics and mathematics. These frameworks automatically apply stencil computations while transforming high-level syntax to machine code and incorporating various optimizations. In contrast, our framework provides an interface that operates at the level of computational abstraction. This approach maximizes productivity by supporting expressive stencil computations without sacrificing optimization opportunities and maintaining code simplicity. Moreover, our framework supports broader backends, including emerging architectures.

4 FRAMEWORK DESIGN AND ARCHITECTURE

The StencilPy framework consists of multiple layers, as illustrated in Figure 2.

The frontend layer enables application developers to express stencil computations using a DSL embedded in Python. The frontend parses the DSL code and converts it into an abstract syntax tree representation.

The optimization layer serves several purposes. First, it applies static and semantic analyses to understand the stencil shape, computation pattern, and data characteristics. The optimization layer employs multiple passes, including

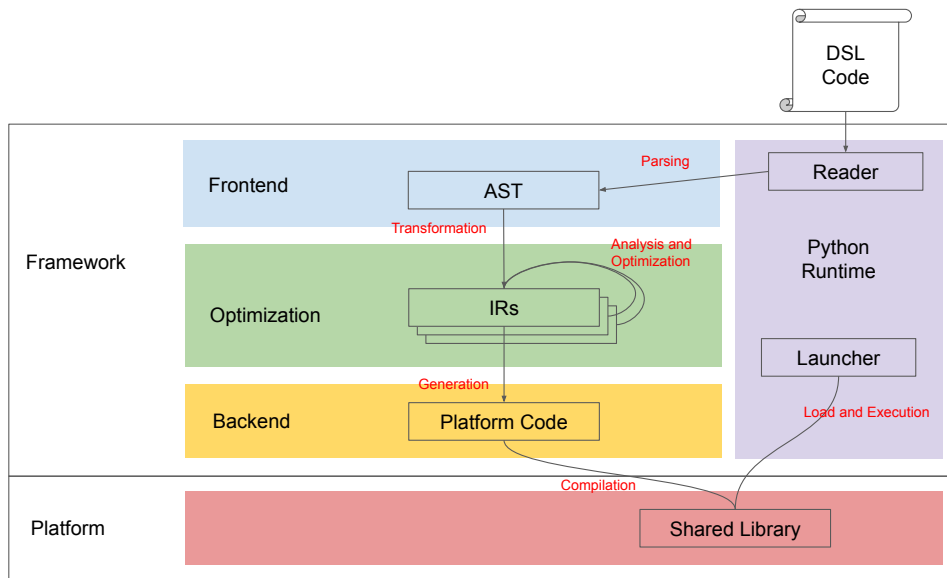


Fig. 2. The StencilPy framework architecture.

decomposition, tiling, reordering, and others to transform the stencil computations by lowering a high-level abstraction to a form optimized for execution on the target backend. Multiple intermediate representations are designed and used during the process to support these transformations.

The backend is capable of producing high-performance code for a range of modern architectures and generates a corresponding code version based on configuration.

Last, the launcher employs Just-In-Time compilation of the code, executes the program, and captures the results.

5 DSL AND FRONTEND DESIGN

Listing 1 depicts an example of a `star2d4r` stencil implementation using the StencilPy framework.

StencilPy’s DSL is hosted in Python by expanding its syntax. Domain scientists commonly use Python because of its simple, high-level syntax. Python is ideal for rapid prototyping. It has an extensive library ecosystem that further enhances its utility. Python’s user-friendly nature contributes to its ease of learning and smooth transition from implementations in other languages. Our DSL is embedded in Python to leverage these pre-existing advantages.

Our DSL distinguishes itself from Python in two areas: 1) we introduce a few constructs specific for stencil computations, and 2) in our constructs, type hints are required.

StencilPy-Specific Constructs. Table 1 shows all constructs and their purposes introduced by the StencilPy framework.

By annotating `@st.target` or `@st.kernel`, the regular Python function declarations become StencilPy targets or kernels, respectively.

Each kernel implicitly defines the indices of the current center point, which is used as a base to offset from in `in` and `at.set` constructs.

A `map` construct takes three argument groups: looping pattern, pointers to the kernels, and kernel parameters. When Perfectly-Matched Layers (PML) [30] present, to support inner region and PML regions, StencilPy takes the looping

```

1 import stencilpy as st
2
3 @st.kernel
4 def kernel_star2d4r(u: st.grid, v: st.grid):
5     v.at(0, 0).set(0.25005 * u.at(0, 0)
6         + 0.11111 * (u.at(-4, 0) + u.at(4, 0))
7         + 0.06251 * (u.at(-3, 0) + u.at(3, 0))
8         + 0.06255 * (u.at(-2, 0) + u.at(2, 0))
9         + 0.06245 * (u.at(-1, 0) + u.at(1, 0))
10        + 0.06248 * (u.at(0, -1) + u.at(0, 1))
11        + 0.06243 * (u.at(0, -2) + u.at(0, 2))
12        + 0.06253 * (u.at(0, -3) + u.at(0, 3))
13        - 0.22220 * (u.at(0, -4) + u.at(0, 4)))
14
15 @st.target
16 def target_star2d4r(u: st.grid, v: st.grid, iter:st.i32):
17     for _t in range(iter):
18         st.map(e=u.shape)(kernel_star2d4r)(u, v)
19         (v, u) = (u, v)
20
21 u = st.grid(dtype=st.f32, shape=(1000,1000), order=4)
22 v = st.grid(dtype=st.f32, shape=(1000,1000), order=4)
23 # data initialization omitted for brevity
24 st.launch(
25     backend=st.cuda(
26         computeCapability="9.0",
27         threadsPerBlock=(16, 8, 8),
28         template=st.CUDABackend.Template.gmem,
29     )
30 )(target_star2d4r)(u, v, 1000)

```

Listing 1. A star2d4r stencil implementation using StencilPy.

Construct	Purpose
kernel	A compute kernel on device. It is typically the stencil loop.
target	Host logic to set up the computations and launch kernels. Usually, this is the time loop for stencil iterations.
map	Looping the multi-dimensions in a data grid, and maps a kernel to each stencil point.
launch	Specifies the backend used in the stencil computation, optimization strategies employed in the simulation, and launches the target.
at	Reads a point value based on the offset indices from the current stencil point.
at.set	Updates a point value based on the offset indices.
grid	A data array used to store a stencil data grid.

Table 1. StencilPy DSL constructs.

pattern explicitly defined with the begin and end indices of the inner region and PML regions. In addition, to improve developer expressiveness, the framework provides syntactic sugar for common use cases where the region boundaries can be inferred from the stencil data grid. For example, the map call in Listing 1 shows a pattern that loops through the whole grid determined by the shape of the u grid.

To support various backends, when launching a target, backend-specific parameters are provided in a backend object. Listing 1 shows an example of launching a backend leveraging the CUDA programming model. This example

sets its compute capability to 9.0, running on an NVIDIA H100 GPU. The `threadPerBlock` defines the GPU block dimensions, and `template` specifies which code generation template to use. In this example, it is a global memory template. The framework currently bundles the backends and their respective templates for sequential execution, OpenMP, CUDA, HIP, SYCL, and CSL programming models. A later section describes each of them in detail.

To facilitate development, debugging, and evaluation, the `launch` construct takes additional optional parameters not shown in Listing 1. For example, `--print-code` outputs generated code to terminal, `--save-temps` preserves all intermediate code in a subdirectory of `/tmp`, and `--profile` measures the time spent in different framework components, including code parsing, generation, compilation, and execution.

Type Hints Required. Python is a dynamically typed language. While its types are only checked and validated at runtime, for us to generate correct code with our backends, type information needs to be known at compile time. Furthermore, type information can be important in analyzing code for performance optimization opportunities. Therefore, while type hints are optional in Python, StencilPy requires type hints in its `kernel` and `target` constructs.

6 FRAMEWORK IMPLEMENTATION AND OPTIMIZATION

The StencilPy framework includes components in Python and C. The frontend of the framework is implemented in Python, handling the parsing of the DSL. The rest of the framework, including optimizations and backend code generation, is implemented in C. C language is known for its efficiency and simplicity, making it mostly suitable for efficient code execution while maintaining readability and ease of maintenance. It operates at the right level for our purpose without introducing excessive processing overhead.

The interaction between Python and C code is facilitated using Python's `ctypes` library and several dynamically-linked libraries compiled from the C code. This approach enables the necessary functionality without introducing extra overhead that could impact execution performance. Moreover, because `ctypes` is built-in to Python, the framework doesn't require any extra third-party dependencies, facilitating the use of the framework on different platforms for better developer accessibility.

Unlike running kernels based on programming models such as OpenMP or CUDA, where the code needs to be compiled ahead of time (AOT), and then executed on the compiled binaries, Python, being an interpreted language, enables users to run their code directly with Just-in-Time (JIT) compilation. This shortens the feedback cycle and enables faster development iterations. We want to preserve this user experience, so under the hood, despite the backend generating code that requires compilation, the framework employs JIT compilation.

While Python is portable, its interpreters are still platform-specific. However, the details are transparent to end users. Users only need to install the binaries for their platform and start using the tool. StencilPy adopts the same approach to maximize portability and enhance user experience. This also supports the common practice in scientific application development, where applications are initially developed on laptops or small-scale workstations, using a sequential backend or consumer-grade accelerators, and later evaluated on HPC clusters.

Allocating, accessing, and looping through large-size data grids in Python is not designed to be fast. For example, in one of our development machines with a modern Intel Xeon CPU, populating a data grid of 1000^3 with random 32-bit floating-point values in Python runtime takes approximately six minutes. In response, StencilPy has its C-based data layer implementation for better performance. Nevertheless, despite being implemented in C, the data layer is exposed as a Python module using `Python.h` interface, seamlessly integrated into Python runtime with no third-party dependencies.

Furthermore, our data layer provides commonly used data array operations, supplemented by stencil-specific operations. These stencil-specific operations are handled differently depending on whether they operate on the host machine or the device. When computing on a host, the framework directly executes the operators implemented in our data layer. To compute on a device, the framework generates device-specific code. Then, the framework compiles and executes the generated code on the target device.

The framework generates platform-specific code based on the provided backend configuration and, if needed, a C interface. This code is then compiled and assembled into a shared library. The shared library can then be loaded and executed with *ctypes* by the framework.

7 STENCIL PERFORMANCE OPTIMIZATIONS

To accelerate runtime performance, StencilPy’s optimizers employ a range of parameters that control code analysis and generation. While the long-term goal is to introduce an auto-tuner with a cost model to pick the best configurations, in the current version, users manually provide all these parameters, with certain parameters inferred by the framework. For the inferred configurations, the framework allows them to be overwritten by users, providing flexibility in customization and can be helpful in cross-compilation scenarios.

Table 2 provides an overview of all the parameters supported by the framework. These parameters can be categorized into three groups: environment parameters, domain-specific parameters, and user-guided performance-tuning parameters. Most of these optimizations are detailed in previous chapters, and others will be discussed later when we discuss the intermediate representation design and code generations.

8 WORKFLOW

This subsection describes the framework’s internal workflow – how a piece of stencil code goes through our framework and eventually runs on the hardware.

The process begins with domain developers writing kernels in the DSL. The DSL code is parsed into an Abstract Syntax Tree (AST). The AST is then transformed into the highest level of intermediate representations (IRs). While the AST is represented using Python’s data structures, the intermediate representations use C-based data structures.

The IRs undergo an analysis phase to infer various properties of the stencil kernel. Static analyses are applied to understand the stencil computations and stencil data arrays. In the first phases of IR transformations, the framework annotates the IR with additional information that represents the stencil kernel, such as stencil shape, looping pattern, stencil grid updates, local variables, and others, making it easier for optimization. Next, the IR goes through multiple optimization phases. Based on user-provided performance tuning parameters, the IR is manipulated and optimized using a suite of optimization techniques. Then, architecture-specific information is utilized to optimize the kernel further. This process eventually generates an IR optimized for performance and designed to facilitate code generation.

Depending on the target architecture, the IR is fed into a platform-specific code generator. The code generator transforms it into target source code dedicated to a programming model or a particular architecture. For example:

- For AMD, Apple, IBM, and Intel CPUs, *ompgen* generates C code with OpenMP directives;
- For Fujitsu A64FX, *ompgen* generates a specialized OpenMP code with configurations dedicated to the Fujitsu compiler;
- For NVIDIA GPUs, *codagen* generates CUDA code and its C interface;
- For AMD GPUs, *hipgen* generates HIP code and C interface;

	Inferred by kernel definition	Available at the call site
Environment parameters		Device traits, such as device type, model, memory size, bandwidth, shared memory model or distributed memory model, memory hierarchy or flat memory, core frequency, etc); Host information; etc.
Domain parameters	Stencil orders; Stencil shapes, such as star, compact-in-space, and box; Stencil data array properties, such as number of elements, grid dimensions, memory locales, etc.	Problem domain size; PML layer width; Looping patterns; Number of iterations; etc.
Performance guidance parameters	Domain decompositions, such as unified, two-region, and seven-region; Loop unrolling; Paddings to the innermost dimension and/or the 2D plane; global memory read with coalescing; etc	<p><i>CPUs</i>: OpenMP configurations, such as using loops, collapsed loops, tasks, looptask, etc. Applying Semi-stencil algorithm [12, 13];</p> <p><i>GPUs</i>: Tiling strategies, such as 3D tiling and 2.5D tiling, and their respective parameters for variants, such as number of time steps, tile sizes; Algorithm choice, such as simple 3D mapping, streaming variants as in Nguyen [44], Micikevicius [42], and Matsuoka [39]; Semi-stencil [12, 13] on the streaming dimension; Data buffering related, such as whether to employ <code>memcpy_async</code> if hardware supports it, number of planes to buffer; Hardware-specific features, such as vectorized data types (<code>float4</code>); etc.</p> <p><i>STX</i>: Utilizing hardware features, such as plane-scheme.</p> <p><i>Cerebras</i>: PE private memory saving strategies; Using <code>memcpy</code> for accelerating host-device data transfer; Using asynchronous communications for inter-PE data movements; vectorization of floating-point operations.</p>

Table 2. StencilPy performance-tuning parameters.

- For Intel GPUs, `syclgen` generates SYCL code;
- For STX, `stxgen` generates OpenMP code with STX’s custom OpenMP extension;
- For Cerebras, `cs1gen` generates CSL code and its Python runner.

In addition, the framework also has a basic code generator `cgen` to generate serial code in C.

Finally, the backend-specific runner compiles and executes the generated code. For all but Cerebras backends, the runners invoke platform-dedicated compilers to build and assemble the code into shared libraries. The shared libraries are then loaded and executed. For Cerebras, the framework generates multiple CSL files for stencil computations, task and state management, and fabric layout. These CSL files are compiled into multiple executable files in ELF using `cs1c` compiler. Finally, `cs_python`, a Cerebras-specialized Python, distributes these ELF files onto either Cerebras hardware or simulators and moves data between host and device for execution.

After the execution, the results are stored in the memory spaces in our data layer so that the program can inspect them or provide them to enclosing code.

Configuration	Description
loop	Uses a runtime schedule and applies an OpenMP <code>parallel</code> for to the outermost loop.
loop_blocking	Adopts a runtime schedule and uses blocking in the outermost two dimensions with OpenMP <code>parallel</code> for applied to the 2D loop nest over the blocks.
loop_blocking_collapse	In addition to the configuration of <code>loop_blocking</code> , applies <code>collapse(2)</code> to combine the two loops.
tasks_blocking	Uses blocking in the outermost two dimensions and runs each block as an OpenMP <code>task</code> .
taskloop	Applies a <code>taskloop</code> to the loops, runs each chunk of iterations as a <code>task</code> .

Table 3. Strategy templates for OpenMP backend on a 3D stencil.

9 BACKEND TEMPLATES

StencilPy supports seven backends, namely `seq` (for sequential code), `omp` (for OpenMP), `cuda`, `hip`, `sycl`, `stx` (for STX-specific OpenMP code generation), and `cs1` (for Cerebras CS-2). The framework includes template(s) specific to each backend, serving as the basis for code version variations. Depending on the domain problem and backend, developers can experiment with templates and their variants for the best performance. Most templates come with parameters, allowing for customization. Developers can tweak these “knobs” to tune the performance.

9.1 Sequential Backend (`seq`)

The most basic backend executes the DSL in a single-threaded fashion using a single CPU core. It supports most CPU architectures, such as ARM, IBM POWER, and x86. It provides one template with no parameters. The main purpose of offering such a template in the framework is to establish a baseline for numeric results and sequential execution performance.

9.2 OpenMP Backend (`omp`)

The framework provides OpenMP backend for code versions utilizing OpenMP programming models. It offers templates for two stencil shapes: conventional stencil computation and Semi-stencil, respectively. For each of the stencil shapes, the backend provides five OpenMP configurations as depicted in Table 3. In total, StencilPy can produce OpenMP code variants of ten combinations of two stencil shapes and five OpenMP configuration strategies.

Table 3 outlines the OpenMP configurations, and for the ones using blocking strategies (`loop_blocking`, `loop_blocking_collapse`, and `tasks_blocking`), StencilPy provides parameters to configure the sizes of the 2D block dimensions.

These code versions and their optimizations are intended to support modern many-core CPUs, such as the HPC nodes sporting AMD EPYC GenoaX, Fujitsu A64FX, IBM Power9, and Intel Sapphire Rapids. Besides, they can be used to speed up the local development of kernels on multi-core CPUs, such as AMD Ryzen, Apple Silicon, and Intel Core.

To cater to a diverse range of platforms, the OpenMP backend carries optimal compilation configurations, including the type of compiler, compiler frontend flags, and linker flags. The default values of these configurations are provided by the framework’s frontend, ensuring that the backend utilizes them to achieve the best performance on the specific platform. However, users can overwrite these configurations or provide new configurations as part of the backend clause.

Template	Description	Blocking
gmem	3D blocking using global memory only	3D
smem	3D blocking using shared memory for stencil grids	
f4	3D blocking using global memory and float4 data type for vectorized computations	
shift	2.5D streaming, data on the streaming dimension are “shifted” when streaming to the next plane	2.5D
unroll	2.5D streaming, data on the streaming dimension are “fixed” using loop unrolling	
semi	2.5D streaming using Semi-stencil algorithm	

Table 4. Built-in templates for GPU backends on a 3D stencil.

9.3 GPU Backend (cuda, hip, and sycl)

GPU vendors have their respective programming models, but they are similar for the most part, although the details differ. Table 4 presents all the built-in templates for 3D stencils tailored on GPU backends, including CUDA, HIP, and SYCL.

3D-blocking templates parameterize block size along the X , Y , and Z axes. Similarly, templates of 2.5D blocking parameterize plane sizes for their X and Y dimensions.

When specified using `--mem-type` flag, 2.5D-blocking templates generate code using registers or shared memory for stencil points on the streaming dimension. Furthermore, when no memory type is specified, the framework automatically selects the memory type based on the stencil shape, with star-shaped stencils employing registers and other stencil shapes employing shared memory. This is possible because the framework identifies the stencil shape in the analysis and optimization phase.

In addition, prefetching can be enabled for 2.5D templates using `-prefetch` flag, enabling data fetching to overlap with computations. Lastly, when hardware support is present, `-asyncmemcpy` flag can be set to move data without staging through registers, freeing registers to be used by computations. This option is currently available to CUDA backend that runs on the latest generations of NVIDIA GPUs.

The GPU templates also support 2D stencils with everything described but one dimension lower.

9.4 STX Backend (stx)

The framework comes with three templates for STX: `cube`, `plane`, and `semi`. STX templates are limited to 3D stencils due to STX toolchain restrictions. The `cube` template resembles GPU’s 3D blocking. The `plane` template aligns with STX’s plane scheme. The `semi` template applies the Semi-stencil algorithm on top of the plane scheme. Both cube sizes and plane sizes can be adjusted with parameters for performance tuning.

9.5 CSL Backend (csl)

There are unique features in the dataflow architecture of the Cerebras CS-2 compared to conventional platforms. As a result, hand-crafting CSL code is time-consuming and error-prone, and many optimizations employ CSL’s special features that harm code readability and make it harder to maintain. To our knowledge, StencilPy’s CSL backend is the first attempt to address these issues, enabling developers to write high-level stencil code and use a framework to handle the CSL code generation and optimization for the CS-2. Although CSL backend has a single template with no parameter, it significantly lowers the barrier to using a Cerebras system for stencil-based computations.

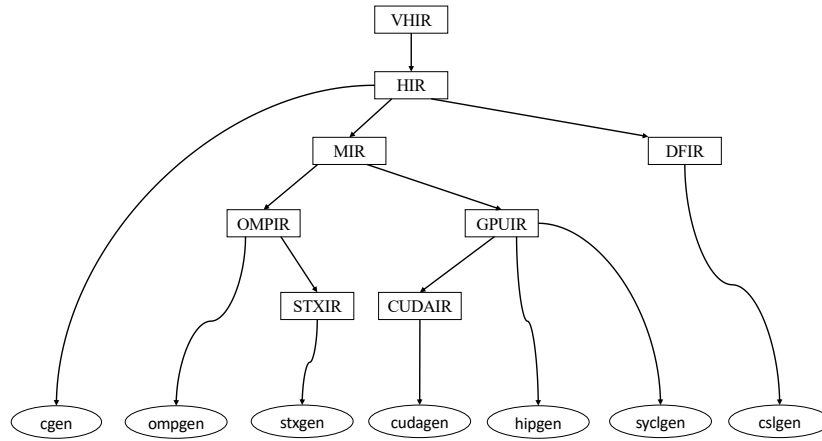


Fig. 3. IR hierarchy in StencilPy framework.

We believe the framework’s built-in templates for each backend cover a comprehensive range of high-performance algorithmic approaches and optimizations for high-order stencils, drawing inspiration from prior research. Nonetheless, should the built-in templates not align with the needs of a specific domain application, developers can extend the framework by introducing new templates to the backend, thanks to the backend template system’s modular design. When working with a new architecture, it is also quite straightforward to introduce templates for backends and “plug-in” them into the framework. Throughout StencilPy’s development, we have applied this methodology to developing all backends.

10 INTERMEDIATE REPRESENTATIONS

Many of StencilPy’s features, such as code generation support for a wide range of backends using various templates and performance optimizations, rely on static analysis. StencilPy’s static analysis comprehends the code and considers it from multiple perspectives. To facilitate static analysis in StencilPy, it employs a multi-layer intermediate representation (IR).

Unlike IR designs used by compiler toolchains for general-purpose languages that must preserve source locations and maintain higher-level semantics, the sole goal of StencilPy’s IR is to support the generation of highly performant code that runs on modern node architectures.

Figure 3 depicts our IR hierarchy. Higher-level IRs are closer to the syntactic abstraction of the DSL, while lower-level IRs are closer to machine code abstractions. In each static analysis phase, the framework transforms these IRs from higher to lower.

10.1 VHIR

VHIR sits at the top of the hierarchy and represents the same information as the DSL’s AST. This is the interface between the framework’s Python models and C data structures.

10.2 HIR

The framework traverses the VHIR, extracts the information about the stencil involved in computation and its data domain, and yields an HIR.

At this level, the framework analyzes data regions, identifying the boundaries of data subregions. The framework examines stencil computations to understand their radius and data grid dimensions. Synthesized from grid data and PML sizes, the framework infers the loop details, including the number and size of loop dimensions and the looping patterns. Furthermore, it comprehends the stencil patterns related to point locations by identifying index offsets involved in computations, assessing the dimensionality of the stencil, and determining whether those points are perfectly aligned on the cardinal axes or not.

HIR is used directly by `cgen`, which generates serial code.

10.3 MIR

MIR incorporates annotations for blocking strategies, such as whether 3D stencils should employ 3D blocking or 2.5D blocking, and for 2D stencils, whether to utilize 2D blocking or 1.5D blocking. MIR maintains a lightweight symbol table, recording local variables and the information around the variables, such as its position at the kernel's top level, whether its right-hand side involves a stencil update, whether it functions as a temporary variable, or if it serves as the destination for a stencil update.

While no code generator directly consumes MIR, it serves as a base IR for both GPU-IR and OMPIR and contains shared information used by both children IRs.

10.4 GPU-IR

GPU-IR concerns details related to GPU-specific hardware features, such as global memory, shared memory, constant memory, and registers. It determines optimal strategies for data storage, access, and movement among these memory types on a GPU device.

In cases where the prefetch configuration is on, GPU-IR calculates the additional memory buffer necessary for prefetching.

Additionally, when the specified GPU sports vectorization units, GPU-IR transforms regular floating-point types into `float4` data types for efficient vectorization.

GPU-IR possesses sufficient information suitable for direct input into `hipgen` and `syclgen`, while `cudaGen` can use some extra information for its processing.

10.5 CUDA-IR

NVIDIA has introduced an asynchronous memory copy feature in their latest A100 and H100 GPUs, enabling data movement without staging through registers. Since asynchronous memory copy doesn't need registers during data prefetching, they can be utilized for overlapping computations concurrently, leading to improved performance. When asynchronous memory copy is enabled, CUDA-IR notes it to take advantage of these features.

To accommodate all recent generations of NVIDIA GPUs, GPU-IR retains information about the current device's compute capability. This ensures that `cudaGen` employs the new asynchronous memory copy feature when supported by the device and falls back to the conventional approach when it is not.

10.6 OMPIR

OMPIR understands looping patterns, including the number of dimensions and whether it directly loops on data grid dimensions. Additionally, it considers whether and how to iterate over a block when accounting for variations in blocking strategies when `loop_blocking`, `loop_blocking_collapse`, and `tasks_blocking` templates are employed.

OMPIR is the input for `ompngen`. It also serves as a basis for STXIR.

10.7 STXIR

The STX programming model extends OpenMP with architecture-specific extensions. OpenMP still manages computations on its host CPU, while the extension introduces nested offloading, specifically addressing offloading tasks to STX processing units. [56] STXIR annotates the on-device computation and inserts device memory allocation and data movement between the host and device. With STX-specific information annotated, STXIR is ready to be consumed by `stxngen`.

10.8 DFIR

Dataflow architecture has unique features, so DFIR needs to handle many aspects, such as data mapping on a processing element (PE), data movement between host memory and device memory, data communication among PEs, and vectorization of the stencil computation. To coordinate computation and distributed asynchronous data communications, synthesized from the stencil computation, DFIR dynamically constructs a state machine for each program execution. Each state machine defines information such as the data preparation, communication, and computation for each stencil point, the current state, and the next state for each state. The state machine receives asynchronous callbacks and decides when to move to the next state. DFIR also introduces stencil point index patterns to facilitate the management of the state machine and data dependency. We delve into stencil point index patterns in detail in this subsection, while deferring the discussion on state machine generation to when we describe code generation for the CSL backend.

Derived from HIR with additional stencil and data grid-related information, DFIR is annotated with details such as the symbol list and stencil point index patterns. The symbol list is crucial for exposing the symbol interface, enabling data flow between the host and the device. Stencil point index patterns provide essential information about the offset, distance, and location relationships in stencil computations, influencing state management, data communication patterns, and vectorization.

We annotate DFIR with hardware information, including fabric dimensions, requested PE width and height based on stencil grid size, and the layout of activated PEs within the fabric. We also allocate buffer PEs for data to flow from and to the host.

Typically, it is straightforward to incorporate the total time iterations into the target. However, in the context of dataflow architecture, where total time iterations and current iteration are integral parts of state machine management, it is required for the total time steps to be known during compilation, thus, is recorded in DFIR.

Stencil grid mapping onto a WSE wafer involves decomposing the data domain, with each Z-dimension cell mapped to the same PE, and X and Y dimensions spread across the wafer axes as shown in Figure 4. The whole Z-dimension resides in the local memory of a PE. This strategy, as demonstrated in previous work [28, 52, 55], optimizes the utilization of dataflow architecture and maximizes the potential parallelism for HPC applications of this kind. The stencil grid's width and height are constrained by maximum PE dimensions, while its depth is limited by PE's private memory size. So, they are also annotated in DFIR.

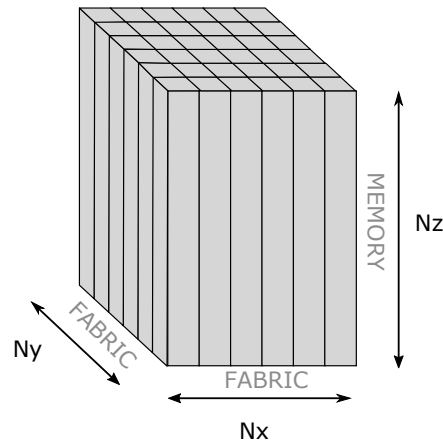


Fig. 4. 3D grid of size $N_x \times N_y \times N_z$. X and Y dimensions are mapped onto the PE grid of the WSE, while Z dimension is mapped onto memory of each PE.

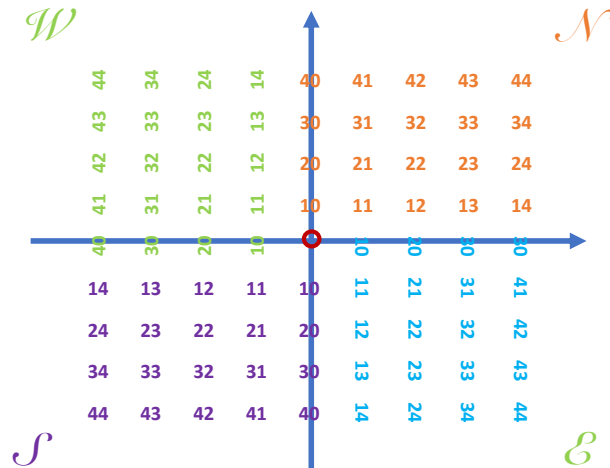


Fig. 5. Stencil point index pattern used in DFIR and CSL code generation.

In Figure 5, we present the structure of our stencil point index patterns for a stencil with a radius of four. The center position is labeled as pattern identifier \emptyset . Other positions in each quadrant are uniquely identified based on their offset from the center point. By analyzing the stencil pattern in computations, we map the stencil offset index to the corresponding stencil point index pattern identifier. Each quadrant is labeled with a directional tag. For instance, quadrant I is denoted as N , II as W , III as S , and IV as E . The identifiers for each pattern do not carry numeric significance. Instead, they are labeled to enhance readability – the tens digit indicates the offset along the axis from the center point, while the ones digit indicates the distance from the perpendicular axis. Rotating the index patterns counterclockwise in the N quadrant provides the index patterns for the other three quadrants. Moreover, the indices associated with each axis are linked to a specific quadrant. Algorithm 2 outlines the procedure for mapping a stencil point’s offset to a

Input:

x, y, z : index offset from center point of x, y , and z dimension, respectively

Output:

id : stencil point index pattern identifier

```
if  $x = 0 \wedge y = 0$  then
```

```
  |  $id \leftarrow 0$ ;
```

```
else
```

```
  switch ( $x, y$ ) do
```

```
    case ( $\geq 0, > 0$ ) do  $d \leftarrow N, i \leftarrow y, j \leftarrow x$ ;
```

```
    case ( $> 0, \leq 0$ ) do  $d \leftarrow E, i \leftarrow x, j \leftarrow -y$ ;
```

```
    case ( $\leq 0, < 0$ ) do  $d \leftarrow S, i \leftarrow -y, j \leftarrow -x$ ;
```

```
    case ( $< 0, \geq 0$ ) do  $d \leftarrow W, i \leftarrow -x, j \leftarrow y$ ;
```

```
  end
```

```
   $id \leftarrow d \oplus i \oplus j$ ;
```

```
/*  $\oplus$  denotes string concatenation */
```

```
end
```

Algorithm 2: Mapping stencil offset index to a stencil point index pattern identifier.

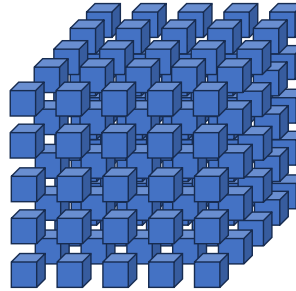


Fig. 6. Shape of a 3D box-shaped stencil with a radius of two.

stencil point index pattern identifier. Parallel data communication can be achieved for the stencil points sharing the same index pattern identifiers from different quadrants.

Subsequently, we provide an example to illustrate the concept of stencil point index pattern and its mapping algorithm. Figure 6 shows the stencil points in a 3D box-shaped stencil with a radius of two. Upon applying Algorithm 2, the resulting mapping is depicted in Figure 7.

The stencil point index pattern is formulated in 2D to conceptually align with the fabric's 2D layout. As the entire Z -dimension is contained within the local memory of a PE, the stencil point index pattern is annotated with the maximum Z -dimension offset. Algorithm 3 describes the process of annotating a stencil point index pattern with its associated maximum Z -dimension offset.

Because a PE router only connects to the routers of its four cardinal directly neighboring PEs, for data communication, pattern 10 in any quadrant can send data to the center point using the router links directly. In contrast, all other patterns need to indirectly send data to the center point, relying on one or more other patterns from the same quadrant to complete prior to its own communication. For example, pattern N20 depends on pattern N10, pattern E30 depends on pattern E20 then indirectly depends on pattern E10, and pattern W22 cascades depends on patterns W21, W20, and W10.

W22	W12	N20	N21	N22
W21	W11	N10	N11	N12
W20	W10	0	E10	E20
S12	S11	S10	E11	E21
S22	S21	S20	E12	E22

Fig. 7. Stencil point index pattern identifiers for the stencil in Figure 6.

Input:

a: an array of stencil offset indexes
id: stencil point index pattern identifier

Output:

m: maximum Z-dimension offset for the provided id

$m \leftarrow 0$;

foreach (x, y, z) *in a do*

$pid \leftarrow$ apply Algorithm 2 with (x, y) ;

if $pid = id$ **then**

if $z > m$ **then**

$m \leftarrow z$;

end

end

end

Algorithm 3: Annotating a stencil point index pattern identifier with its associated maximum Z-dimension offset.

Consequently, depending on the data's location in the stencil computation, DFIR conducts data analysis, constructing a dependency array using the steps described in Algorithm 4 for data communications from these stencil point index patterns. Figure 8 provides the dependency graph for the example stencil depicted in Figure 6. This dependency array is subsequently used to generate code that controls the router to choreograph the sending and receiving of data. It also manages the state machine and tracks progress to ensure that data communications adhere to the specified dependency order.

Finally, DFIR transforms the numeric operations in a stencil computation from a tree data structure into a Static Single Assignment (SSA) [11] form based on stencil point index patterns. It is needed for generating vectorized code.

DFIR is the input to `cs1gen`, which generates CSL code.

11 CODE GENERATION

Our code generators produce platform-specific source code, leveraging platform compilers to generate machine code tailored to the target architecture. For instance, `cuda` generates CUDA code, using `nvcc` to produce the corresponding NVIDIA GPU machine code. Similarly, `cs1gen` generates CSL code, and `cs1c` is employed to generate an ELF executable for Cerebras systems. Given our framework's goal of transforming a user-friendly stencil DSL into efficient code, it is best to reuse existing platform-specific infrastructure instead of reinventing the wheel. Therefore, our code

Input:

a: an array of stencil offset indexes

Output:

s: sorted dependency array of a

Function DependsOn(*id1*, *id2*):

```

dep ← false ;                               /* if id1 depends on id2, return true */
d1 · i1 · j1 ← id1 ;
d2 · i2 · j2 ← id2 ;                         /* extracts d, i, j from id */
if d1 ≠ d2 then
  | dep ← false ;                             /* patterns from different quadrants never depend on each other */
else
  | if j1 = j2 then
    | dep ← i1 > i2 ;
  | else
    | dep ← j1 > j2 ;
  | end
  | end
  | end
end
return dep ;
end

```

s ← sort a using DependsOn as the comparison function ;

Algorithm 4: Constructing dependencies among stencil point index patterns.

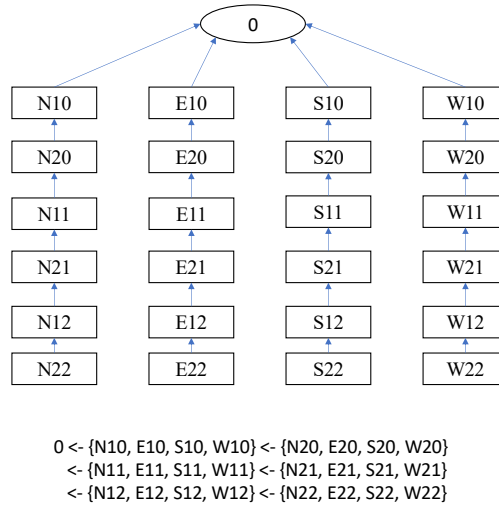


Fig. 8. Stencil point index pattern dependency for the stencil in Figure 6.

generators produce the code in such a way that allows us to delegate certain traditional compiler optimizations to the platform-specific compilers, enabling us to concentrate on stencil optimizations.

In general, each code generator accepts an IR as input and produces code for stencil kernels as well as target code for launching the kernels. They generate code to map the data region to the kernel where the stencil computation

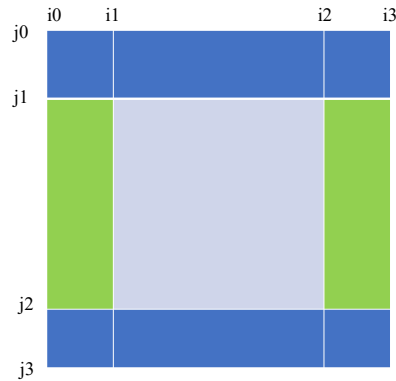


Fig. 9. 2D decomposition defined with map construct.

occurs. They also handle memory allocation on the host. Additionally, some code generators generate C interfaces for interaction with the framework frontend.

11.1 Serial Code (cgen) and Commonly Shared Code Generation

cgen takes HIR and generates serial versions of the code in C. While this process is straightforward, it serves as an opportunity to extract commonly shared code generation logic that can be reused in other code generators.

For instance, the generation of primitive numeric types, such as `int` and `float`, can be reused across different code generators. Similarly, the generation of most numeric operators (including prefix and binary operators) and control flow logics (such as `if-else` statements and `for` statements) can be shared among all code generators except `cs1gen`.

Regarding for statements, the DSL adopts Python's `for-range` loop syntax, so the framework converts it to a C for loop with an initial condition, termination condition, and incremental statement.

Shared logic also includes stencil index arithmetic. The DSL defines stencil points based on offsets from an implicitly defined current stencil point index, while its data structure is flattened to a 1D data array in host memory. Halo regions are part of the physical memory layout, so the arithmetic between the two indexing systems is implemented here and can be reused.

Additionally, the logic for handling data decomposition and launching kernels according to decomposed data regions can be reused. Figure 9 illustrates a 2D decomposition using boundary indices as defined in DSL code `map(i=(i0, i1, i2, i3), j=(j0, j1, j2, j3))`. The framework provides syntactic sugar to accommodate common use cases, such as

- `map(i=x, j=y)` is translated to `map(i=(0, 0, x, x), j=(0, 0, y, y))`;
- `map(i=x, j=y, w=p)` to `map(i=(0, p, x-p, x), j=(0, p, y-p, y))`;
- `map(i=(x1, x2), j=(y1, y2))` to `map(i=(x1, x1, x2, x2), j=(y1, y1, y2, y2))`;
- `map(i=(x1, x2), j=(y1, y2), e=p)` to `map(i=(x1, x1+p, x2-p, x2), j=(y1, y1+p, y2-p, y2))`;
- `map(e=(x, y))` to `map(i=(0, 0, x, x), j=(0, 0, y, y))`; and
- `map(e=(x, y), w=p)` to `map(i=(0, p, x-p, x), j=(0, p, y-p, y))`.

Although parentheses are used in the DSL syntax, it's important to note that all intervals are semantically left-closed and right-open. The 3D decomposition is similar but includes a third parameter k to define the decomposition for the Z-dimension.

11.2 OpenMP Code Generation (`ompgen`)

In addition to generating common workflow and reused code, `ompgen` primarily focuses on three aspects of OpenMP-specific code generation: kernel code, blocking strategies, and various OpenMP pragmas for different configurations.

For kernel code, `ompgen` generates one of two code versions based on the backend parameter: one using conventional stencil computation and the other applying the Semi-stencil algorithm.

Depending upon the blocking strategies implied by the chosen template, `ompgen` either produces code with looping patterns that iterates through the entire data grid or decomposes the data grid into blocks and loops over the block dimensions. The loop dimension lengths are determined by the data grid, while the block dimensions are provided as backend template parameters.

The selected template also determines how `ompgen` incorporates OpenMP pragmas into the code.

- `#pragma omp parallel for default(shared) schedule(runtime)` is applied to all loop-based templates, including `loop`, `loop_blocking`, and `loop_blocking_collapse`. The `loop` template applies them to the outer loop, while `loop_blocking` and `loop_blocking_collapse` apply them to 2D blocks. `loop_blocking_collapse` further applies `collapse(2)` to collapse 2D blocks;
- For the `tasks_blocking` template, `#pragma omp parallel default(shared)` and `#pragma omp master` are applied to the outer loop over time iterations, where `#pragma omp task` is applied to the inner loop over 2D blocks. `ompgen` also adds a `#pragma omp taskwait` at the end of the timestep; and
- if the `taskloop` template is used, `#pragma omp parallel default(shared)`, `#pragma omp single`, and `#pragma omp taskloop` are applied to the outer loop.

11.3 GPU Code Generation (`cuda`, `hip`, and `sycl`)

While GPUs from the three major vendors have their respective programming models, GPU code generation shares some commonalities. We describe the common elements applicable to all three GPU code generators, and when variations arise, we address their differences.

The initial step in GPU code generation involves generating code for the allocation of data arrays in on-device memory. The stencil data grid is flattened into a 1D array layout. Padding between rows and lead padding to adjust the initial offset of each row are added to the memory layout to align inner region blocks with cache lines. Subsequently, code is generated to copy data from the host to the device. The generated data facilitates data copying with memory coalescing.

Next, code generators create GPU kernels and generate the corresponding kernel launch calls. In addition to launching kernels with the data decomposition previously described, when offloading kernels to GPUs, they generate code to instruct the allocations of GPU threads and threadblocks, as part of the kernel launch calls. GPU threadblocks are determined by the blocking strategies implied by the chosen template.

Both `cuda` and `hip` generate code to allocate streams for CUDA and HIP, respectively, and launch kernels on these streams. On the other hand, `sycl` produces a `submit` call and uses its command group handler to dispatch kernels onto devices.

The generation of kernel code is primarily decided by the kernel definition, selected template, and its parameters. In templates using 3D blockings, the first step involves determining the stencil center point index that the current thread handles. For both CUDA and HIP, this computation relies on implicitly-defined variables such as `blockIdx`, `blockDim`, and `threadIdx`, while `syclgen` can easily obtain the index from a `nd_item`.

For the `gmem` template, code generation is straightforward. The generated code retrieves stencil point values directly from device memory, performs the computation, and directly updates the results in the device memory.

In the case of the `smem` template, the process requires several steps. First, code is generated to allocate shared memory space for CUDA and HIP, and `local_accessor` for SYCL. Subsequently, stencil indices in both global memory layout and shared memory layout are generated. Following this, code is generated to load data from global memory to shared memory. Finally, stencil computation code is generated with data being read from shared memory. The updated stencil value is then updated in device memory.

The `f4` template is similar to `gmem` in that it retrieves data directly from global memory. However, the key difference lies in each GPU thread concurrently computing four floating-point numbers using its vector engine. The code generation involves converting the stencil index to the components of `float4` (x , y , z , and w). The stencil computation uses data from `float4` types to vectorize the computation. Subsequently, the generated code updates four values in global memory. In the `f4` template, the challenge is to ensure that the stencil index is accurately mapped to the current `float4` instance and its components. While manually writing vectorized code can be error-prone, using a compiler-assisted approach like the StencilPy framework significantly simplifies this process. The framework not only eases the development of vectorized code but also enhances performance through efficient vectorization of computations.

Transitioning to templates employing 2.5D blocking, the code generators must determine the stencil point index relative to the 2D plane being streamed. Next, depending on the template and its parameters (`-memory-type` and `-prefetch`), they must generate code for data allocations in various memory types, including shared memory and registers. Additionally, code is generated to set the initial values in these memory spaces before generating the streaming loop.

All 2.5D templates generate a `for` statement or `while` statement iterating from the beginning streaming index to the end. During each streaming step, code is generated to prepare data in all memory types for the stencil computations of the current plane. Then, careful code generation ensures the stencil computation is performed using stencil points from the correct locations in different memory types. Once the stencil computation is completed, the results for that plane are stored back in global memory. In the case where `-prefetch` is enabled, additional code is generated to fetch the data for the next plane, while overlapping stencil computation on a prior plane.

When preparing data for the current plane after streaming down to a new plane, the `shift` template rotates values in memory space to position them correctly for the new plane index. On the other hand, the `unroll` and `semi` templates use loop unrolling to keep existing data stationary in their memory locations while loading new data to the appropriate positions. In hand-crafted code versions, we use macro preprocessing to achieve loop unrolling. However, StencilPy's code generators can directly generate the expanded code.

The `semi` template requires additional code generation for both the forward phase and the backward phase of the Semi-stencil algorithm. It also generates code for allocating spaces for partial results and subsequently managing these partial results according to the Semi-stencil algorithm during computations.

When `-asynccopy` flag is on, and the compute capability in CUDAIR satisfies, `cudaGen` produces memory copy code using `__pipeline_memcpy_async`. Additionally, `__pipeline_commit` and `__pipeline_wait_prior` are also properly generated.

Lastly, correct device synchronization and thread synchronization are essential, and the code generators manage these processes appropriately.

11.4 STX Code Generation (`stxgen`)

`stxgen` first needs to decompose the data domain into smaller data regions. The size of a region is subject to the hardware-specific quota of `TCDM_SIZE`, which is the size of the memory on an STX cluster. Subsequently, for each of these regions, `stxgen` generates code to request an STX cluster and offload the respective data region to it.

Next, it generates code for allocating data arrays in the TCDM memory of the STX cluster and copies data from the host to the cluster.

Then, for the cube template, the code generation introduces `#pragma omp target` to the entire stencil kernel and a nested `#pragma stx worksharing(interleave)` to the outer loop of the data region. The first pragma specifies the section of the code that executes on the cluster, while the latter pragma offloads the stencil computation of the entire 3D cubic data region to the STX Processing Units (SPUs) on the cluster. After generating code for the stencil computation, `stxgen` generates code to transfer data back to the host from TCDM.

The plane template generates code aligned with STX's plane scheme design. The plane scheme closely resembles the 2.5D blocking in GPUs, with the SPU accelerating streaming index arithmetic at the hardware level. It incorporates an asynchronous DMA engine, enabling concurrent, non-interfering data transfers and computations similar to the asynchronous memory copy in the latest NVIDIA GPUs.

For plane, the code generation adds `#pragma omp parallel num_threads(2)` and checks the OpenMP thread ID. STX's OpenMP extension reserves ID 0 for logic running on the host and ID 1 for code offloading to the STX cluster. Thus, `stxgen` produces code that checks the OpenMP thread ID and generates code for host and device, respectively.

For the host thread, `stxgen` generates code to transfer the stencil results from the previous streaming step stored in TCDM back to host memory. Additionally, the generated code for the host prefetches the data for the upcoming streaming plane and stores it in the buffer.

For the cluster thread, the generated code employs both `#pragma omp target` and a nested `#pragma stx worksharing(interleave)` to the stencil computations for the current plane. The generated code adheres to the plane scheme design, facilitating the overlap of data transfer with stencil computations.

Finally, `stxgen` generates the code that adds `#pragma omp barrier` to the end of each streaming step, ensuring synchronization among all SPUs and data transfers.

Next, the semi template is based on plane template that builds on top of the concept of the plane scheme. However, during stencil computation, instead of the conventional stencil approaches, the Semi-stencil algorithm is applied. Additionally, when generating the code for data array allocations, additional spaces are required in TCDM for partial results. Note that data transfer between the host and the device is unnecessary for partial results since they are exclusively used in stencil computations and can remain in TCDM. During the generation of code for the cluster thread, the template incorporates the Semi-stencil algorithm into the streaming dimension. It conducts a forward computation across the entire streaming plane, storing partial results, followed by a backward computation using these partial results. The final results are stored in TCDM, and the host thread can copy them from TCDM to the host memory in the coming streaming iteration.

Finally, following the offload section, all templates generate code to release the memory allocated on the requested STX clusters.

11.5 CSL Code Generation (`cs1gen`)

The dataflow architecture makes CSL code generation challenging. Generating code involves controlling router configurations, managing data communications, vectorizing the stencil computation, defining the state machine and transitions, and structuring the code layout while exposing symbols.

Controlling Router Configurations. First, `cs1gen` generates code defining a routing plan that involves a sequence of switch positions for the router in a PE. Route designs are typically straightforward, involving actions such as receiving from one direction, sending to the opposite direction, and utilizing Ramp link to communicate with the enclosing PE. The route design for each of the four directions is independent and could vary. For PEs at the edge of the PE grid, route design can be more intricate, requiring careful handling of cases when a PE may only send or receive in certain directions.

In addition to route design, `cs1gen` must generate code instructing routers to switch their positions, enabling data to flow through and to its destination. This is accomplished using a CSL construct known as control wavelet. Therefore, `cs1gen` produces code for control wavelets and generates code to dynamically trigger these events, facilitating the switch of router positions.

Managing Data Communications. Having generated router code, `cs1gen` proceeds with code generation for data communications utilizing these router configurations.

Figure 5 shows how DFIR represents data communication using stencil point index patterns. Following the application of Algorithms 2 and 4, DFIR incorporates all stencil point index patterns and their dependencies for the current stencil computation. Algorithm 5 depicts how to convert an array of stencil point index patterns with sorted dependency to data communications.

For each pattern, `cs1gen` generates code choreographing the data transfer. Certain data transfers may involve multiple steps that involve intermediate routers, and these are handled accordingly by state management. Additionally, some data transfers depend on the completion of communication for other stencil point index patterns, and these dependencies are also addressed in the state management.

For a 3D box-shaped stencil with radius of two as depicted in Figure 6, upon the application of Algorithm 5, Table 5 illustrates the data communication actions involved in each iteration.

Vectorizing the Stencil Computation. To accelerate stencil computation on a Cerebras system, vectorization of computations is essential. This is achieved by using Data Structure Descriptors (DSDs) and `builtin`s provided by the Cerebras SDK. A DSD is a compact representation of a set of data elements, which may be non-contiguous. A `builtin` performs a bulk operation on a DSD's elements, leveraging a single hardware instruction to vectorize computations. The Cerebras SDK bundles `builtin`s supporting various numeric operators, including addition, subtraction, multiplication, multi-adds, and logical operations.

Based on the stencil computation, `cs1gen` produces DSDs describing the memory access for the stencil grid involved in the computation. Subsequently, it generates numeric operations using the provided `builtin`s. Given that DFIR already represents the computation in Static Single Assignment (SSA) form, `cs1gen` simply needs to map operations to `builtin`s.

Defining the State Machine and Transitions. The state machine serves as the glue for all subcomponents, tracking states and coordinating their transitions. It manages the preparation of sending data, the actual data transfer, the destination

Input: *patterns*: an array of stencil point index patterns computed and sorted using Algorithms 2 and 4, respectively

Function *Send*(*d*, *i*, *j*):

```

    d' ← switch d do
    |   case E do return West; case N do return South;
    |   case W do return East; case S do return North;
    end
    switch (i, j) do
    |   case (1, 0) do Send 0 to d';
    |   case (1, j) where j ≠ 0 do
    |       | sourceId ← d ⊕ j ⊕ 0;                               /* ⊕ denotes string concatenation */
    |       | d'' ← switch d do
    |       | |   case E do return North; case N do return West;
    |       | |   case W do return South; case S do return East;
    |       | end
    |       | Send sourceId to d'';
    |       end
    |       otherwise do
    |           | sourceId = d ⊕ (i - 1) ⊕ j;
    |           | Send sourceId to d';
    |       end
    |   end
    end
    foreach id in patterns do
    |   d · i · j ← id;                                       /* extracts d, i, j from id */
    |   Send(d, i, j);
    |   do ← switch d do
    |       |   case E do return East; case N do return North;
    |       |   case W do return West; case S do return South;
    |       end
    |       Receive from do into id;
    end
end

```

Algorithm 5: Transforming sorted stencil point index patterns to data communications.

for received data, the arrival of all data required for stencil computation, the execution of stencil computation, the tracking of the current time iteration, and the termination of execution at the end of the time iterations. *cs1gen* also generates and manages states for the whole program execution, including its setup and teardown.

We show the generated states and illustrate state transitions using an example of a 3D box-shaped stencil with a radius of two, as depicted in Figure 6. This example assumes a straightforward stencil update with all coefficients set to one in each iteration. We iterate the stencil updates 1000 times for demonstration purposes.

First, *cs1gen* generates three states: *STATE_SETUP*, *STATE_TEARDOWN*, and *STATE_EXIT*. *STATE_SETUP* prepares the execution preparation, during which the timer is started. *STATE_TEARDOWN* finishes the execution, stopping the timer. Moreover, *STATE_TEARDOWN* prepares the buffers for the final results, including the stencil data arrays and the profiling data, allowing their transfer back to the host. *STATE_EXIT* places the fabric in its final state and signals the host to start receiving the final results.

	N		E		S		W	
	Send Action	Receive Action	Send Action	Receive Action	Send Action	Receive Action	Send Action	Receive Action
Step 1	Send 0 to South	Receive From North into N10	Send 0 to West	Receive from East into E10	Send 0 to North	Receive from South into S10	Send 0 into East	Receive from West into W10
Step 2	Send N10 to South	Receive From North into N20	Send E10 to West	Receive from East into E20	Send S10 to North	Receive from South into S20	Send W10 into East	Receive from West into W20
Step 3	Send N10 to East	Receive From North into N11	Send E10 to South	Receive from East into E11	Send S10 to West	Receive from South into S11	Send W10 into North	Receive from West into W11
Step 4	Send N11 to South	Receive From North into N21	Send E11 to West	Receive from East into E21	Send S11 to North	Receive from South into S21	Send W11 into East	Receive from West into W21
Step 5	Send N20 to East	Receive From North into N12	Send E20 to South	Receive from East into E12	Send S20 to West	Receive from South into S12	Send W20 into North	Receive from West into W12
Step 6	Send N12 to South	Receive From North into N22	Send E12 to West	Receive from East into E22	Send S12 to North	Receive from South into S22	Send W12 into East	Receive from West into W22

Table 5. Data communication actions involved in each iteration for a 3D box-shaped stencil with radius of two (Figure 6).

```

1 @st.kernel
2 def kernel_box3d2r(u: st.grid, v: st.grid):
3     v.at(0, 0, 0).set( # a box3d2r stencil update assuming coefficients of ones
4         u.at(-2, 0, 0) + u.at(-2, -2, -2) + u.at(-2, -2, -1)
5         + u.at(-2, -2, 0) + u.at(-2, -2, 1) + u.at(-2, -2, 2)
6         + ... # omitted for brevity
7     )
8
9 @st.target
10 def target_box3d2r(u: st.grid, v: st.grid):
11     for _t in range(1000):
12         st.map(e=u.shape)(kernel_box3d2r)(u, v)
13         (v, u) = (u, v)

```

Listing 2. Example code for iterating a simple update for a 3D box-shaped stencil with a radius of two as in Figure 6.

DFIR contains information regarding the dependencies among stencil point index patterns. Consequently, `cs1gen` generates code defining the states necessary for these stencil point index patterns and produces code facilitating transitions among these states based on their dependencies. For each index pattern, `cs1gen` generates two states, `STATE_PREP_TRANS_id` and `STATE_TRANS_id`, for preparing and initiating the data transfers, respectively. `STATE_PREP_TRANS_id` loads the data being transferred to a dedicated data buffer and makes it available to the router. On the other hand, `STATE_TRANS_id` activates the router to enable the data flow into the router links. Once all data has been piped into the links, it controls the router switches to start receiving data, which is then stored into the appropriate data buffer. Algorithm 5 outlines this transformation. For the example of a 3D box-shaped stencil, `cs1gen` generates the following states:

- STATE_PREP_TRANS_10,
- STATE_TRANS_10,
- STATE_PREP_TRANS_20,
- STATE_TRANS_20,
- STATE_PREP_TRANS_11,
- STATE_TRANS_11,
- STATE_PREP_TRANS_21,
- STATE_TRANS_21,
- STATE_PREP_TRANS_12,
- STATE_TRANS_12,
- STATE_PREP_TRANS_22, and
- STATE_TRANS_22.

Besides, `cs1gen` generates two more states, `STATE_UPDATE_STENCIL` and `STATE_ITERATION_CHECK`, to execute the actual stencil computation and perform time iteration checking, respectively. Control statements such as ternary operators and if-else statements are also converted into states, transforming conditionals into explicit state transitions. For instance, in the stencil computation depicted in Listing 2, which iterates 1000 times, `cs1gen` generates code in `STATE_ITERATION_CHECK` such that if the currently processed iterations are less than 1000, it transitions to `STATE_PREP_TRANS_10`; otherwise, it transitions to `STATE_TEARDOWN`.

In addition to generating all the states, `cs1gen` also produces code that handles state transitions. We assume the entire state machine always starts with `STATE_SETUP`. Upon the setup step finishes, it transitions to the first state generated based on stencil point index pattern dependencies. In our example of the 3D box-shaped stencil, this is `STATE_PREP_TRANS_10`. Once the state machine progresses through all data communication states, the last communication state transitions to `STATE_UPDATE_STENCIL`. In our example, upon the completion of `STATE_TRANS_22`, it transitions to `STATE_UPDATE_STENCIL`. Upon finishing the stencil update for this iteration, it transitions to `STATE_ITERATION_CHECK`. Depending on the iteration count, it either returns to `STATE_PREP_TRANS_10` for data communication and stencil computation for the next iteration, or it transitions to `STATE_TEARDOWN` to wrap up the execution. Finally, it transitions to `STATE_EXIT` to conclude the state machine transitions.

Structuring the Code Layout While Exposing Symbols. Lastly, `cs1gen` generates a layout file that instructs the Cerebras runtime on the distribution of the ELF binaries. It creates code that petitions a rectangular fabric region for ELF execution. Each PE within the requested region specifies the generated CSL source file containing router configurations, data communication, stencil computations, and the state machine. It sets up the initial state of the program execution.

Additionally, the code generator produces instructions for exposing symbols, enabling the host to access pointers to either data buffers or functions. Exposing data buffers to the host facilitates the transfer of data to or from the fabric, while function pointers enable the host to invoke them, initiating the state machine and receiving callbacks upon its completion.

12 CUSTOMIZATIONS AND EXTENSIONS

StencilPy's modular design supports customization and extension at various levels, including parameterized backend, derivative backend, implementing new launchers for existing backends, and introducing new templates and backends.

12.1 Parameterized Backend

Built-in backends are parameterized to allow configuration of framework behaviors at compile and/or run time as discussed in Section 7.

12.2 Derivative Backend

The framework supports derivative backends, enabling the modification or minor extension of an existing backend. This concept is similar to creating a subclass in object-oriented programming, where derived backends can be inherited from an existing backend. Derived backends define overridden behaviors or introduce new behaviors, adapting them to the existing backend behavior.

For instance, in the context of the dataflow architecture, our CSL backend currently supports the Cerebras CS-2 system with behaviors tailored to that specific machine using their SDK version 1.0.0, such as allocating extra PEs used as buffers for host-to-device data communications. SDK version 1.0.0 allocates extra three, one, four, and one PEs to the north, east, south, and west boundaries, respectively. If the sizes of these extra PE allocations ever change due to machine upgrades or SDK updates, one can introduce a derived backend. This derived backend can either overwrite these configurations or set both the PE dimensions and fabric dimensions directly without significantly altering the framework.

12.3 New Launchers

The framework supports the addition of new launchers, enabling alterations in the way kernels are launched or supporting new hardware by reusing existing generated code while executing it with configurations dedicated to the new hardware.

For example, our SYCL backend is presently designed for data center-grade Intel discrete GPUs with dedicated on-device memory. SYCL, being a cross-platform abstraction layer, also supports GPUs from NVIDIA and AMD, CPUs, and FPGAs. If there's a requirement to reuse the generated SYCL code but launch it on these alternative platforms, one can effortlessly implement new launchers. The framework maintains the same SYCL configuration and code generation, leveraging the new launcher to execute binaries on these diverse platforms.

12.4 New Templates and Backends

The framework's modular design facilitates its extension through the introduction of new templates to an existing backend and the implementation of entirely new backends for future architectures. The framework supplies the HIR and all configuration parameters to a backend. Interfaces for code generators and launchers are also provided. Common IR and shared code generation utility functions are extracted into internal libraries to ease code reuse.

For those looking to implement their own backend, any of our built-in backends can serve as an example. This approach also streamlines the process and ensures consistency in extending and implementing custom backends within the framework.

13 EVALUATIONS

This section describes our evaluation, starting with the numerical accuracy of the generated code. Then, we use a 3D 25-point star-shaped stencil to evaluate its runtime performance. Next, we quantitatively demonstrate the developer productivity boost accomplished by using the framework.

Kernel	Stencil Shape	Dimension	Stencil Order	FLOPs
star2d1r	Star	2D	1	9
star2d2r			2	17
star2d3r			3	25
star2d4r			4	33
star3d1r		3D	1	13
star3d2r			2	25
star3d3r			3	37
star3d4r			4	49
box2d1r	Box	2D	1	17
box2d2r			2	49
box2d3r			3	97
box2d4r			4	161
box3d1r		3D	1	53
box3d2r			2	249
box3d3r			3	685
box3d4r			4	1457
j2d5pt	Star	2D	1	10
j2d9pt-gol	Box	2D	1	18
j2d9pt	Star	2D	2	18
j3d27pt	Box	3D	1	54

Table 6. Kernels for numerical correctness evaluation

Our evaluation covers all existing backends and templates that are built-in to the current version of the framework.

13.1 Numerical Accuracy

The framework can generate backend code for various orders and of different shapes, so to evaluate the numerical accuracy of the generated code on various backends, we assembled a suite of kernels commonly used in stencil computations based on stencils described by Matsumura et al. [38]. These kernels encompass a wide range of variations in terms of stencil characteristics found in scientific applications.

Table 6 provides an overview of these kernels and highlights the properties of interest for our evaluations. We have included both star-shaped and box-shaped stencils, as well as commonly used stencils like those found in Jacobian matrices. Our evaluation includes both 2D and 3D stencils, with stencil orders ranging from 1 to 4.

For the STX backend, since 2D kernels are not supported by STX toolchain, only 3D kernels are evaluated. Moreover, although 2D stencils can be evaluated for the Cerebras backend, they represent the least efficient utilization of the hardware. Therefore, we exclude them from our evaluation as they lack practical significance.

Although we are confident that our `cs1gen` generates correct code for `box3d3r` and `box3d4r` kernels, the `cs1c` compiler crashes internally during frame lowering. We have reported the issue to the vendor, but in this study, we have omitted their evaluations.

To assess numerical accuracy, our framework processes these kernels and generates multiple code versions using different backends, templates, template customizations, and optimization parameters. We designed the experiment to be comprehensive to cover all variants of our code generators. We generate many code versions for each backend. The numbers of generated code versions for each backend are:

- seq: 20
- omp: 200
- cuda: 648
- hip: 348
- sycl: 348
- stx: 21
- csl: 7

The evaluation runs a total of 1592 code versions to check the numerical accuracy. In our evaluation, we automate the comparison of results of kernels generated with StencilPy against a separately hand-crafted reference OpenMP implementation to verify numerical accuracy.

For the result of each stencil point, we define an error as the absolute numerical difference between a kernel generated with StencilPy and the reference OpenMP implementation. We find the maximum error and calculate the root-mean-square deviation (RMSD) of all errors for the entire stencil data grid. The values involved in the computation range from 10^{-4} to 10^5 . Our max errors for these comparisons are in the range of 10^{-7} , while RMSDs are in the magnitude of 10^{-8} , proving good numerical accuracy of our code generation.

13.2 Runtime Performance and Portability

To evaluate the StencilPy framework in terms of performance, portability, and productivity using real-world scientific applications, we present a 25-point star-shaped stencil used in the acoustic isotropic approximation of the wave equation [41] (Acoustic ISO). Previous works by Raut et al. [47], Sai et al. [56, 58, 59], and Jacquellin et al. [9, 28] present manually developed code versions for CPUs, GPUs, STX, and Cerebras, respectively. In this study, we implement the Acoustic ISO stencil using the StencilPy DSL, and we use the hand-crafted versions as reference implementations. For a fair comparison, we also rerun the evaluations on our hardware with newer software stacks.

We compare the overall *time-to-solution* of code generated by StencilPy with that of hand-crafted code. This includes execution time both on the host and on the accelerator, if any. For StencilPy, time-to-solution includes the cost of parsing and code generation.

To facilitate the performance evaluation of code generated by StencilPy, we added a built-in profiler to the framework. This profiler collects and reports performance metrics, including time for code parsing, code generation, compilation, data movements between host and device, execution on devices, etc.

13.2.1 CPUs. For CPU evaluations, we first present results using a MacBook Pro laptop and then discuss two data-center-level many-core CPU devices: AMD EPYC 9684X and Fujitsu A64FX.

Apple M1 Max. First, we present the time measurement results on a MacBook Pro equipped with the Apple Silicon M1 Max chip. Despite being a laptop designed for consumer use and lacking data-center-level hardware features, it serves as one of our development machines during tool development. Therefore, the performance results on Apple Silicon offer insights into the average user experience for typical scientific application developers.

The M1 Max chip employs an ARM-based architecture. The M1 Max used in our development and evaluations hosts eight performance cores with a maximum frequency of 3.2 GHz and two efficiency cores clocked at 2.06 GHz. The machine is equipped with 32 GB of RAM. The code compilation uses Apple Clang version 15.0.0, an Apple-specific Clang distribution integrated into macOS' development toolchains.

Due to memory size constraints, we conduct runs with a grid size of 500^3 . The evaluation runs 1000 time iterations. The time measurement results are detailed in Table 7. All time measurements are presented in seconds.

Configurations			StencilPy				Manual Code
Template	Semi	Compiler	Frontend	Code Gen	Kernel	Time to Solution	Time to Solution
loop	N	Clang	0.0031	0.0742	72.6357	72.7131	70.6608
loop_blocking			0.0029	0.0007	58.6567	58.6603	60.6297
loop_blocking_collapse			0.0030	0.0008	47.0523	47.0561	48.8303
tasks_blocking			0.0029	0.0007	46.7118	46.7153	45.9665
taskloop			0.0029	0.0007	69.2095	69.2132	66.7804
loop	Y		0.0029	0.0009	86.2431	86.2469	81.5342
loop_blocking			0.0029	0.0009	101.0792	101.0830	85.1640
loop_blocking_collapse			0.0029	0.0010	75.8235	75.8273	70.5379
tasks_blocking			0.0029	0.0009	78.0275	78.0314	64.0150
taskloop			0.0031	0.0009	83.8647	83.8688	76.9300

Table 7. Time measurements on a Macbook Pro laptop with Apple Silicon M1 Max chip.

The overall time to solution from StencilPy-generated code is comparable to that of manual code. The overhead introduced by the framework remains relatively low, negligible when compared to the overall time to solution. Consequently, the iteration time for a developer to assess a code change with a substantial data grid size is less than two minutes, a feedback cycle deemed quite reasonable and normal in daily practices.

AMD GenoaX. We conducted evaluations on a system equipped with an AMD EPYC 9684X CPU of 192 cores. The machine is configured with 750 GB of RAM. The evaluation environment supports both GCC 8.3.1 and Clang 17.0.0 compilers, so our experiments assess both compilers. To ensure fair comparisons, our runs are conducted with a grid size of 500^3 and time iterations of 1000.

The results of time measurements are outlined in Table 8. All time measurements are in seconds. The overall time to solution from StencilPy-generated code mostly aligns with that of manual code. Notably, in certain configurations — such as applying the taskloop template on the Clang compiler, combining the loop template with the Semi-stencil algorithm on the Clang compiler, and many configurations employing the GCC compiler — StencilPy-generated code demonstrates superior performance compared to the manual code.

The variation in performance impact among different compilers stems from the fact that OpenMP is an open standard, and each compiler has its own internal implementations. Consequently, our results reveal disparities in performance when using different compilers. For instance, in our results, regardless of whether generated by StencilPy or manually written, the GCC compiler produces suboptimal machine code compared to the Clang compiler. Specifically, when utilizing the loop_blocking template with the Clang compiler, regardless of whether applying Semi-stencil or not, the manual code exhibits faster execution than the StencilPy-generated code. However, when employing the same configurations with the GCC compiler, while both run slower, manual code execution demonstrates significant performance degradation and becomes slower than StencilPy-generated code.

Fujitsu A64FX. We assessed the A64FX backend on a system equipped with 48 A64FX cores and 32 GB RAM. To accommodate memory size constraints, our runs were conducted with a grid size of 500^3 . Each run iterates 1000 times.

Configurations			StencilPy				Manual Code
Template	Semi	Compiler	Frontend	Code Gen	Kernel	Time to Solution	Time to Solution
loop	N	Clang	0.0033	0.0009	20.1053	20.1095	20.4953
loop_blocking			0.0033	0.0008	34.6278	34.6319	17.3618
loop_blocking_collapse			0.0033	0.0008	11.3075	11.3116	9.9881
tasks_blocking			0.0033	0.0008	34.6857	34.6899	27.8640
taskloop			0.0034	0.0009	27.6730	27.6773	32.2575
loop	Y		0.0034	0.0011	17.8976	17.9021	22.2907
loop_blocking			0.0033	0.0010	42.5678	42.5722	29.3809
loop_blocking_collapse			0.0033	0.0011	13.7320	13.7364	12.2444
tasks_blocking			0.0034	0.0011	29.5314	29.5359	26.2103
taskloop			0.0035	0.0011	31.1501	31.1547	30.5132
loop	N	GCC	0.0032	0.0007	28.8949	28.8988	32.5906
loop_blocking			0.0032	0.0008	50.6335	50.6375	119.2601
loop_blocking_collapse			0.0032	0.0008	26.6967	26.7008	32.1390
tasks_blocking			0.0033	0.0008	90.8078	90.8118	41.7210
taskloop			0.0033	0.0008	25.3038	25.3079	31.6666
loop	Y		0.0033	0.0010	30.3951	30.3993	35.7536
loop_blocking			0.0032	0.0010	61.2420	61.2462	161.7382
loop_blocking_collapse			0.0033	0.0010	25.4091	25.4134	30.2028
tasks_blocking			0.0033	0.0011	81.1837	81.1880	94.4311
taskloop			0.0033	0.0011	25.9430	25.9474	30.6635

Table 8. Time measurements on an AMD GeonaX CPU

The evaluations employed FCC, a proprietary Fujitsu compiler tailored with optimizations specifically designed for the Scalable Vector Engine (SVE) integrated with the A64FX chip. FCC is provided as part of Fujitsu Software Compiler Package V1.0L21, and Python is from anaconda3 v2021.05.

Table 9 shows our framework generates code suffers a performance decline compared to the manually crafted code. Although its overhead is still deemed negligible in the context of the entire execution time, it appears to be higher than that of other backends.

We tentatively attribute the performance degradation to the machine’s outdated software stack, as similar behavior is not observed on other platforms. Its Python setup may also be somewhat incompatible with Fujitsu toolchains. However, further investigations are required to gain a more confirmative understanding towards these unexpected outlier observations.

13.2.2 GPUs. We conducted our evaluations across multiple generations of AMD, Intel, and NVIDIA GPUs. For NVIDIA GPUs, we evaluated on V100, A100, and two H100 GPUs. One H100 GPU is part of an NVIDIA Grace Hopper H200 Superchip and has HBM3e device memory, while the other is a PCIe Gen5 version with HBM2e device memory. For AMD GPUs, we evaluated on AMD MI100 and MI210 GPUs. Our evaluations also include Intel Iris P580 and Max 1100

Configurations			StencilPy				Manual Code
Template	Semi	Compiler	Frontend	Code Gen	Kernel	Time to Solution	Time to Solution
loop	N	FCC	0.0178	0.0361	59.6969	59.7507	85.2817
loop_blocking			0.0176	0.0029	88.5776	88.5981	47.8229
loop_blocking_collapse			0.0178	0.0022	79.1602	79.1802	66.9843
tasks_blocking			0.0178	0.0023	42.9798	42.9998	36.7312
taskloop			0.0181	0.0024	42.4882	42.5087	39.1951
loop	Y		0.0176	0.0038	123.2977	123.3192	103.9921
loop_blocking			0.0176	0.0038	170.0528	170.0743	118.5939
loop_blocking_collapse			0.0177	0.0038	108.8751	108.8967	95.4082
tasks_blocking			0.0176	0.0038	106.2009	106.2223	83.9420
taskloop			0.0181	0.0038	111.6792	111.7012	84.5176

Table 9. Time measurements on A64FX.

	H100 (GH200)	H100 (PCIe)	A100	MI210	Max 1100
CPU	NVIDIA Grace	AMD EPYC 7313	AMD EPYC 7402	AMD EPYC 7402	Intel Xeon 4410T
CPU Cores	72	64	96	96	40
RAM	512 GB	512 GB	512 GB	512 GB	256 GB
GPU	NVIDIA H100	NVIDIA H100	NVIDIA A100	AMD MI210	Intel Max 1100
Cores	16896	14592	6912	6656	56
GRAM	95 GB	80 GB	40 GB	64 GB	48 GB
Platform	CUDA 12.2	CUDA 12.0	CUDA 12.1	ROCm 5.5	OneAPI 2024.0.2
GPU Driver	NV 535.154.05	NV 525.105.17	NV 530.30.02	ROCm 5.5	OneAPI 2024.0.2

Table 10. GPU System specifications.

GPUs. This article only reports results for selected GPUs, namely NVIDIA H100 (GH200), NVIDIA H100 (PCIe), NVIDIA A100, AMD MI210, and Intel Max 1100. Table 10 lists the specifications of these systems and their respective software stacks. We refer to these systems by their GPU models.

To evaluate performance on the H100 (GH200), H100 (PCIe), A100, MI210, and Max 1100 GPUs, we measured the execution time of 1000 iterations. We run different code versions with various configurations. For each 3D template, we run with different 3D tile sizes (Dx, Dy, and Dz); For 2.5D templates, in addition to their 2D plane size (Dx and Dy), they differ by the memory type (Mem Type) used for the values at the streaming dimension and by whether to prefetch coming plane (Prefetching) and overlap the prefetching with computation. For NVIDIA GPUs, we run with and without asynchronous memory copy (Async Mem Cp). In StencilPy evaluations, we report time used for frontend (Frontend), code generation (Code Gen), device execution (Kernel), and total time to solution (Time to Solution). For executions using hand-crafted code, we report its total time to solution (Time to Solution). We consider Kernel to contain the stencil and boundary condition execution times on device. We omit lines where we lack the manual code comparison. All times are in seconds.

Configurations				StencilPy				Manual Code
Template	Dx	Dy	Dz	Frontend	Code Gen	Kernel	Time to Solution	Time to Solution
gmem	8	8	8	0.0036	0.0101	14.3927	14.4065	16.5194
gmem	16	8	8	0.0037	0.0012	12.0103	12.0152	17.0133
gmem	32	4	4	0.0037	0.0012	12.4520	12.4569	10.7388
gmem	32	8	4	0.0036	0.0012	12.6974	12.7022	13.0961
gmem	64	4	4	0.0036	0.0012	12.5346	12.5394	14.0747
f4	8	8	8	0.0037	0.0013	10.3117	10.3167	11.1101
f4	16	8	8	0.0037	0.0013	9.1801	9.1851	13.1615
f4	32	4	4	0.0037	0.0013	9.0773	9.0823	10.5181
f4	32	8	4	0.0036	0.0013	9.4307	9.4357	12.9856
f4	64	4	4	0.0037	0.0013	9.4900	9.4950	13.9485
smem	8	8	8	0.0036	0.0014	16.3265	16.3315	17.6632
smem	16	8	8	0.0037	0.0014	17.1052	17.1104	18.2645
smem	32	4	4	0.0037	0.0014	15.6389	15.6440	10.8190

Table 11. Time measurements for 3D templates on H100 (GH200).

NVIDIA H100 (GH200), H100 (PCIe), and A100. Our evaluation executed each kernel with a grid size of 1000^3 on NVIDIA GPUs. Time measurements for 3D and 2.5D templates on the H100 (GH200) GPU are presented in Tables 11 and 12, respectively. Similarly, time measurements for 3D and 2.5D templates on the H100 (PCIe) GPU are provided in Tables 13 and 14, respectively. Corresponding time measurements for 3D and 2.5D templates on the A100 GPU are showcased in Tables 15 and 16, respectively.

For 2.5D templates, Tables 12 and 14 compare various 2D plane sizes on two H100 GPUs, while Table 16 emphasizes the impacts of utilizing the asynchronous memory copy on the A100 GPU. Additionally, we present the same set of kernels for the two H100 GPUs to demonstrate the influence of high-bandwidth memory updates in the H100 (GH200) version.

Overall, our generated code performs similarly to hand-crafted code. Across all three GPUs, the fastest StencilPy code version applies the f4 template. On the H100 (GP200), the fastest kernel employing the f4 template with a block size of $32 \times 4 \times 4$, resulting in a 15.81% speedup compared to the fastest manually-written CUDA kernel. Meanwhile, the fastest f4 kernels on both the H100 (PCIe) and A100 adopt a block size of $16 \times 8 \times 8$, yielding a 9.49% speedup on the H100 and a 6.92% speedup on the A100 compared to the best manually-written CUDA code performances, respectively. The tables illustrate that the overheads introduced by our framework are minimal. The time required for code analysis and generation is very small and negligible relative to the overall time to solution.

While the performance of the generated code from 3D templates is optimal, templates employing the streaming approach show room for improvement. We believe it is due to the framework generating separate conditionals that guard the initialization of a shared memory copy for each data array, even when the conditionals for each array are

Configurations					StencilPy				Manual Code
Template	Dx	Dy	Mem Type	Prefetching	Frontend	Code Gen	Kernel	Time to Solution	Time to Solution
shift	16	16	registers	N	0.0036	0.0013	19.4624	19.4673	17.7771
shift	16	16	shared memory	N	0.0036	0.0014	19.9392	19.9442	-
shift	16	16	registers	Y	0.0036	0.0014	17.5326	17.5376	13.3297
shift	16	16	shared memory	Y	0.0036	0.0014	17.6369	17.6419	-
shift	32	16	registers	N	0.0036	0.0013	18.1593	18.1642	17.7083
shift	32	16	shared memory	N	0.0036	0.0013	18.9042	18.9092	-
shift	32	16	registers	Y	0.0037	0.0014	16.2037	16.2088	12.0212
shift	32	16	shared memory	Y	0.0036	0.0014	15.5827	15.5877	-
shift	32	32	registers	N	0.0037	0.0013	19.6440	19.6490	19.5460
shift	32	32	registers	Y	0.0036	0.0014	17.6879	17.6929	13.8165
shift	64	16	registers	N	0.0037	0.0031	18.6006	18.6074	20.1936
shift	64	16	registers	Y	0.0036	0.0017	16.7557	16.7610	14.3532
unroll	16	16	registers	N	0.0038	0.0051	19.9793	19.9882	17.4304
unroll	16	16	shared memory	N	0.0037	0.0014	19.9453	19.9505	-
unroll	16	16	registers	Y	0.0037	0.0052	18.1906	18.1994	13.9617
unroll	16	16	shared memory	Y	0.0037	0.0014	17.6382	17.6433	-
unroll	32	16	registers	N	0.0036	0.0049	18.6597	18.6683	16.5325
unroll	32	16	shared memory	N	0.0036	0.0014	18.9013	18.9063	-
unroll	32	16	registers	Y	0.0037	0.0052	17.7084	17.7173	11.5310
unroll	32	16	shared memory	Y	0.0036	0.0014	15.5845	15.5896	-
unroll	32	32	registers	N	0.0037	0.0050	20.0669	20.0756	17.7684
unroll	32	32	registers	Y	0.0037	0.0052	18.8849	18.8938	12.6939
unroll	64	16	registers	N	0.0036	0.0049	19.0538	19.0624	18.7590
unroll	64	16	registers	Y	0.0036	0.0053	18.0072	18.0161	13.2164
semi	16	16	registers	N	0.0036	0.0044	23.0598	23.0678	16.3084
semi	16	16	shared memory	N	0.0037	0.0047	22.8706	22.8789	-
semi	16	16	registers	Y	0.0037	0.0045	19.2181	19.2263	13.9020
semi	16	16	shared memory	Y	0.0037	0.0053	18.0041	18.0131	-
semi	32	16	registers	N	0.0038	0.0044	22.1415	22.1496	17.2477
semi	32	16	shared memory	N	0.0037	0.0048	23.0907	23.0992	-
semi	32	16	registers	Y	0.0036	0.0046	18.8772	18.8854	11.6394
semi	32	16	shared memory	Y	0.0037	0.0053	17.0560	17.0650	-
semi	32	32	registers	N	0.0037	0.0044	27.2095	27.2175	18.4065
semi	32	32	shared memory	N	0.0037	0.0048	25.4199	25.4283	-
semi	32	32	registers	Y	0.0036	0.0046	20.6862	20.6944	12.8455
semi	32	32	shared memory	Y	0.0037	0.0054	19.0712	19.0803	-
semi	64	16	registers	N	0.0037	0.0044	26.1108	26.1189	19.3593
semi	64	16	shared memory	N	0.0037	0.0048	24.5181	24.5266	-
semi	64	16	registers	Y	0.0037	0.0045	19.6786	19.6868	13.3464
semi	64	16	shared memory	Y	0.0037	0.0053	18.0975	18.1065	-

Table 12. Time measurements for 2.5D templates on H100 (GH200).

Configurations				StencilPy				Manual Code
Template	Dx	Dy	Dz	Frontend	Code Gen	Kernel	Time to Solution	Time to Solution
gmem	8	8	8	0.0048	0.0013	24.2196	24.2258	28.6097
gmem	16	8	8	0.0048	0.0024	21.2407	21.2480	27.7491
gmem	32	4	4	0.0062	0.0022	22.8573	22.8656	20.7433
gmem	32	8	4	0.0050	0.0013	22.7887	22.7950	23.3025
gmem	64	4	4	0.0049	0.0019	22.6207	22.6276	24.4729
f4	8	8	8	0.0050	0.0022	19.3295	19.3366	20.2404
f4	16	8	8	0.0049	0.0019	18.2293	18.2362	22.1022
f4	32	4	4	0.0049	0.0016	19.0787	19.0853	19.9678
f4	32	8	4	0.0049	0.0020	19.5722	19.5792	22.3395
f4	64	4	4	0.0050	0.0017	19.3820	19.3887	23.4454
smem	8	8	8	0.0054	0.0017	26.9528	26.9600	28.9192
smem	16	8	8	0.0062	0.0027	26.9418	26.9508	28.8495
smem	32	4	4	0.0048	0.0017	25.8666	25.8731	20.9340

Table 13. Time measurements for 3D templates on H100 (PCIe).

identical. A potential solution involves consolidating the code into a unified set of conditionals. Additionally, another potential performance enhancement is to introduce padding between each row in the memory layout, ensuring that each row aligns with cache lines. This approach was implemented in our manual code versions but is currently missing in StencilPy’s code generator. Both strategies will be explored in our future work.

MI210. Tables 17 and 18 show time measurements for 3D and 2.5D templates on an MI210 GPU, respectively. These results depict the execution duration of each kernel with a grid size of 1000^3 .

The time measurements reveal a pattern similar to those observed with NVIDIA GPUs, highlighting that our generated code performs comparably to manually crafted code. The generated code for 3D templates exhibits speedup, while the one for 2.5D templates demonstrates degradation. We believe that the underlying issues influencing code generation for 2.5D templates remain the same.

The fastest generated code is derived from the gmem template with a block size of $64 \times 4 \times 4$, showcasing a 4.97% speedup compared to the best manually-written HIP code.

Despite improvements with newer compiler and hardware driver versions, we continue to observe suboptimal performance from the 3D blocking kernels with a shape of $8 \times 8 \times 8$, while the performance gaps are being minimized. In addition to addressing the future work outlined in the NVIDIA GPUs subsection, our ongoing efforts also involve engaging with vendors to better understand the issues and explore potential mitigation strategies.

Max 1100. Our evaluation executed each kernel with a grid size of 800^3 on an Intel Max 1100 GPU. Time measurements for 3D and 2.5D templates on the GPU are presented in Tables 19 and 20, respectively.

Configurations					StencilPy				Manual Code
Template	Dx	Dy	Mem Type	Prefetching	Frontend	Code Gen	Kernel	Time to Solution	Time to Solution
shift	16	16	registers	N	0.0049	0.0027	31.3418	31.3493	28.9171
shift	16	16	shared memory	N	0.0050	0.0019	30.5316	30.5385	-
shift	16	16	registers	Y	0.0050	0.0023	27.4088	27.4161	24.5790
shift	16	16	shared memory	Y	0.0051	0.0022	30.6180	30.6252	-
shift	32	16	registers	N	0.0049	0.0023	27.7229	27.7300	27.4469
shift	32	16	shared memory	N	0.0049	0.0022	28.1040	28.1111	-
shift	32	16	registers	Y	0.0049	0.0022	25.1817	25.1887	21.1142
shift	32	16	shared memory	Y	0.0050	0.0023	24.9919	24.9992	-
shift	32	32	registers	N	0.0049	0.0021	29.0632	29.0702	29.9949
shift	32	32	registers	Y	0.0049	0.0024	26.5892	26.5964	22.5614
shift	64	16	registers	N	0.0050	0.0015	27.3358	27.3423	29.6589
shift	64	16	registers	Y	0.0051	0.0023	24.9477	24.9550	22.8828
unroll	16	16	registers	N	0.0050	0.0071	32.0051	32.0173	29.4605
unroll	16	16	shared memory	N	0.0049	0.0022	30.4614	30.4685	-
unroll	16	16	registers	Y	0.0049	0.0077	29.1771	29.1898	26.0431
unroll	16	16	shared memory	Y	0.0048	0.0017	30.7398	30.7463	-
unroll	32	16	registers	N	0.0049	0.0073	28.4429	28.4551	27.0205
unroll	32	16	shared memory	N	0.0051	0.0024	28.1020	28.1095	-
unroll	32	16	registers	Y	0.0049	0.0076	27.5321	27.5447	21.3058
unroll	32	16	shared memory	Y	0.0048	0.0022	24.9946	25.0016	-
unroll	32	32	registers	N	0.0049	0.0071	29.8151	29.8272	28.2825
unroll	32	32	registers	Y	0.0049	0.0073	28.4359	28.4481	21.7548
unroll	64	16	registers	N	0.0049	0.0074	30.7684	30.7807	28.7498
unroll	64	16	registers	Y	0.0053	0.0079	26.8397	26.8528	22.2376
semi	16	16	registers	N	0.0048	0.0061	31.9705	31.9815	28.2321
semi	16	16	shared memory	N	0.0049	0.0070	33.7073	33.7192	-
semi	16	16	registers	Y	0.0049	0.0063	29.7953	29.8065	26.0908
semi	16	16	shared memory	Y	0.0050	0.0082	28.4432	28.4564	-
semi	32	16	registers	N	0.0050	0.0060	29.9796	29.9906	27.8226
semi	32	16	shared memory	N	0.0049	0.0066	32.9409	32.9525	-
semi	32	16	registers	Y	0.0050	0.0065	26.1697	26.1812	21.7486
semi	32	16	shared memory	Y	0.0049	0.0078	26.4207	26.4334	-
semi	32	32	registers	N	0.0050	0.0063	33.9534	33.9648	29.1290
semi	32	32	shared memory	N	0.0051	0.0065	35.9119	35.9234	-
semi	32	32	registers	Y	0.0049	0.0060	27.2581	27.2691	21.7661
semi	32	32	shared memory	Y	0.0052	0.0074	28.6058	28.6184	-
semi	64	16	registers	N	0.0053	0.0063	32.6950	32.7066	28.9953
semi	64	16	shared memory	N	0.0048	0.0066	33.8157	33.8270	-
semi	64	16	registers	Y	0.0048	0.0069	25.3508	25.3626	22.1058
semi	64	16	shared memory	Y	0.0049	0.0072	26.6112	26.6233	-

Table 14. Time measurements for 2.5D templates on H100 (PCIe).

Configurations				StencilPy				Manual Code
Template	Dx	Dy	Dz	Frontend	Code Gen	Kernel	Time to Solution	Time to Solution
gmem	8	8	8	0.0057	0.0013	33.8127	33.8197	34.1936
gmem	16	8	8	0.0057	0.0013	26.6416	26.6485	35.3896
gmem	32	4	4	0.0058	0.0013	30.0117	30.0188	28.0359
gmem	32	8	4	0.0058	0.0013	27.7055	27.7126	29.6036
gmem	64	4	4	0.0058	0.0013	27.5059	27.5129	31.1047
f4	8	8	8	0.0057	0.0014	24.6505	24.6577	24.9756
f4	16	8	8	0.0058	0.0014	22.8316	22.8388	26.3150
f4	32	4	4	0.0058	0.0014	24.4236	24.4308	24.4313
f4	32	8	4	0.0057	0.0014	24.6173	24.6244	26.7922
f4	64	4	4	0.0057	0.0014	24.6714	24.6786	28.2199
smem	8	8	8	0.0058	0.0016	39.1157	39.1230	37.1830
smem	16	8	8	0.0058	0.0015	36.1227	36.1301	34.5510
smem	32	4	4	0.0059	0.0015	39.5155	39.5229	25.0511

Table 15. Time measurements for 3D templates on A100.

We had already switched focus and started working on automated code generation when access to Intel GPU became available, so our effort spent on hand-crafted code versions was limited. While we do not claim that our manual SYCL code is comprehensive or finely tuned, our generated code exhibits a significant speedup compared to the manual code. The most efficient StencilPy code version on the Max 1100 is from the *f4* template with a block size of $16 \times 8 \times 8$.

It is noteworthy that loop unrolling is discouraged in the SYCL programming model [27]. However, both our generated code and manual code for the 2.5D streaming approach heavily rely on it, and thus, has a substantial impact on performance. As part of our future work, we intend to explore code generation using regular for loops to evaluate if this approach can enhance performance.

13.2.3 STX. Table 21 shows time measurements for STX backend using its software simulator. We first show three configurations of the same grid sizes (Grid) and the same block dimensions (Dx, Dy, and Dz) but use different templates. Then, we demonstrate configurations of different block sizes that maximize the TCDM quota. Additionally, we report the respective times used for frontend (Frontend), code generation (Code Gen), code compilation (Comp), simulation time (Kernel), and total time to solution (Time to Solution).

Given the utilization of a software-based simulator, the kernel times are unlikely to represent the actual hardware execution time when it becomes available. Nevertheless, Table 21 highlights that the framework demonstrates minimal overheads, with the frontend and code generation requiring negligible time duration.

It's important to note that, due to the relatively small grid sizes allowed in the software simulator, our evaluation focuses on the inner region, leaving the PML width set to zero.

Configurations						StencilPy				Manual Code
Template	Dx	Dy	Async Mem Cp	Mem Type	Prefetching	Frontend	Code Gen	Kernel	Time to Solution	Time to Solution
shift	32	16	Y	registers	N	0.0058	0.0014	35.3898	35.3970	31.7132
shift	32	16	Y	shared memory	N	0.0058	0.0016	35.7061	35.7134	-
shift	32	16	Y	registers	Y	0.0058	0.0015	32.8403	32.8477	26.0930
shift	32	16	Y	shared memory	Y	0.0058	0.0016	33.1222	33.1296	-
shift	32	16	N	registers	N	0.0058	0.0015	34.6506	34.6578	31.3340
shift	32	16	N	shared memory	N	0.0058	0.0015	36.9580	36.9653	-
shift	32	16	N	registers	Y	0.0058	0.0015	35.7699	35.7772	37.8034
shift	32	16	N	shared memory	Y	0.0058	0.0015	36.7250	36.7323	-
shift	64	16	Y	registers	N	0.0058	0.0014	34.4487	34.4559	36.2959
shift	64	16	Y	registers	Y	0.0058	0.0016	32.8195	32.8268	29.5449
shift	64	16	N	registers	N	0.0057	0.0015	32.9032	32.9104	36.6746
shift	64	16	N	registers	Y	0.0057	0.0016	35.4388	35.4460	40.8021
unroll	32	16	Y	registers	N	0.0057	0.0063	35.9815	35.9936	31.4895
unroll	32	16	Y	shared memory	N	0.0058	0.0015	35.6995	35.7068	-
unroll	32	16	Y	registers	Y	0.0059	0.0068	32.1342	32.1469	24.9978
unroll	32	16	Y	shared memory	Y	0.0058	0.0015	33.1776	33.1849	-
unroll	32	16	N	registers	N	0.0058	0.0066	36.2140	36.2264	31.5686
unroll	32	16	N	shared memory	N	0.0057	0.0015	36.7016	36.7089	-
unroll	32	16	N	registers	Y	0.0058	0.0067	35.9990	36.0115	31.3555
unroll	32	16	N	shared memory	Y	0.0058	0.0015	36.4381	36.4454	-
unroll	64	16	Y	registers	N	0.0057	0.0065	34.7067	34.7189	34.3142
unroll	64	16	Y	registers	Y	0.0060	0.0068	30.8637	30.8765	26.3153
unroll	64	16	N	registers	N	0.0058	0.0063	37.3583	37.3704	34.1682
unroll	64	16	N	registers	Y	0.0057	0.0067	39.0586	39.0710	34.1259
semi	32	16	Y	registers	N	0.0058	0.0056	38.8495	38.8609	32.2854
semi	32	16	Y	shared memory	N	0.0058	0.0063	38.4041	38.4162	-
semi	32	16	Y	registers	Y	0.0059	0.0062	33.0855	33.0976	24.5879
semi	32	16	Y	shared memory	Y	0.0059	0.0073	31.5485	31.5616	-
semi	32	16	N	registers	N	0.0058	0.0056	36.6780	36.6894	32.3097
semi	32	16	N	shared memory	N	0.0058	0.0062	35.4459	35.4579	-
semi	32	16	N	registers	Y	0.0058	0.0060	37.9416	37.9534	31.5952
semi	32	16	N	shared memory	Y	0.0059	0.0072	35.4828	35.4958	-
semi	64	16	Y	registers	N	0.0058	0.0058	42.8673	42.8789	35.0117
semi	64	16	Y	shared memory	N	0.0058	0.0061	40.3642	40.3761	-
semi	64	16	Y	registers	Y	0.0058	0.0057	32.3904	32.4020	26.6811
semi	64	16	Y	shared memory	Y	0.0057	0.0069	32.2965	32.3091	-
semi	64	16	N	registers	N	0.0058	0.0056	39.7020	39.7134	34.9883
semi	64	16	N	shared memory	N	0.0058	0.0060	35.7397	35.7515	-
semi	64	16	N	registers	Y	0.0058	0.0057	39.4307	39.4422	33.5579
semi	64	16	N	shared memory	Y	0.0058	0.0223	35.9052	35.9332	-

Table 16. Time measurements for 2.5D templates on A100.

Configurations				StencilPy				Manual Code
Template	Dx	Dy	Dz	Frontend	Code Gen	Kernel	Time to Solution	Time to Solution
gmem	8	8	8	0.0059	0.0014	267.2109	267.2182	304.7703
gmem	16	8	8	0.0059	0.0014	80.2217	80.2289	89.7744
gmem	32	4	4	0.0059	0.0013	63.1088	63.1161	72.7389
gmem	32	8	4	0.0058	0.0013	56.5997	56.6068	69.4689
gmem	64	4	4	0.0057	0.0014	54.6166	54.6237	62.8044
f4	8	8	8	0.0057	0.0015	153.2549	153.2622	123.8675
f4	16	8	8	0.0058	0.0015	78.4303	78.4376	77.8708
f4	32	4	4	0.0058	0.0015	77.7637	77.7710	74.0969
f4	32	8	4	0.0058	0.0015	78.1449	78.1522	73.0456
f4	64	4	4	0.0058	0.0015	77.1072	77.1145	67.9936
smem	8	8	8	0.0059	0.0017	146.1402	146.1478	147.3259
smem	16	8	8	0.0059	0.0016	68.0168	68.0243	70.2211
smem	32	4	4	0.0057	0.0017	72.1782	72.1856	63.7333
smem	32	8	4	0.0058	0.0016	58.6640	58.6714	58.9743

Table 17. Time measurements for 3D templates on MI210.

13.2.4 *CSL*. Time measurements for the CSL backend are presented in Table 22, and for comparative purposes, additional selected backends are included in the table. We have provided details about the evaluation environments for the other backends, while the CSL backend evaluation is carried out on a Cerebras CS-2 system running Cerebras SDK 1.0.0.

The execution time is measured by iterating the inner region of the Acoustic ISO kernel 10,000 times on each device, utilizing a grid size of $750 \times 994 \times 300$. This grid size maximizes both the on-device memory and computing resources of a Cerebras CS-2. We choose a height of 300 with the assumption that it provides enough space to concurrently store values from each neighboring cell and allocate additional temporary vector buffers needed for vectorization. Our goal is to minimize the number of temporary variables used wherever possible. For a fair comparison, we keep the same grid size for other backends. The unit of measurement in Table 22 is seconds.

The StencilPy-generated CSL code demonstrates performance comparable to hand-crafted code, with negligible overheads. Notably, the CSL backend exhibits a significant speedup compared to other backends.

While technically feasible, having each PE run an independent computation pattern for this type of HPC applications is still uncharted territory. Current best practices for this kind of HPC applications on a dataflow architecture necessitate uniform computation patterns on each PE. Consequently, our evaluation for CSL backend omits the PML layer and focuses solely on the inner region. The evaluation for the entire data grid is a topic for future work.

Configurations					StencilPy				Manual Code
Template	Dx	Dy	Mem Type	Prefetching	Frontend	Code Gen	Kernel	Time to Solution	Time to Solution
shift	16	16	registers	N	0.0059	0.0015	100.6327	100.6401	74.4768
shift	16	16	shared memory	N	0.0059	0.0016	86.4954	86.5029	-
shift	16	16	registers	Y	0.0058	0.0017	97.8574	97.8650	75.0378
shift	16	16	shared memory	Y	0.0058	0.0016	84.4574	84.4648	-
shift	32	16	registers	N	0.0058	0.0015	79.8848	79.8921	59.1248
shift	32	16	shared memory	N	0.0058	0.0016	78.2006	78.2080	-
shift	32	16	registers	Y	0.0058	0.0016	77.4932	77.5007	59.5698
shift	32	16	shared memory	Y	0.0058	0.0017	72.8313	72.8387	-
shift	32	32	registers	N	0.0058	0.0015	78.3407	78.3481	57.6798
shift	32	32	shared memory	N	0.0058	0.0016	67.1130	67.1204	-
shift	32	32	registers	Y	0.0057	0.0016	75.5069	75.5143	57.7668
shift	32	32	shared memory	Y	0.0058	0.0017	61.6610	61.6684	-
unroll	16	16	registers	N	0.0060	0.0069	93.9332	93.9462	72.7401
unroll	16	16	shared memory	N	0.0058	0.0017	86.4164	86.4239	-
unroll	16	16	registers	Y	0.0060	0.0072	95.5166	95.5299	77.4294
unroll	16	16	shared memory	Y	0.0059	0.0016	84.3103	84.3178	-
unroll	32	16	registers	N	0.0059	0.0068	77.1315	77.1442	62.8389
unroll	32	16	shared memory	N	0.0059	0.0017	77.8900	77.8975	-
unroll	32	16	registers	Y	0.0058	0.0071	73.3329	73.3457	66.9978
unroll	32	16	shared memory	Y	0.0061	0.0017	70.9432	70.9510	-
unroll	32	32	registers	N	0.0060	0.0067	76.5835	76.5962	61.5674
unroll	32	32	shared memory	N	0.0058	0.0017	64.8953	64.9027	-
unroll	32	32	registers	Y	0.0058	0.0073	76.0669	76.0800	66.3721
unroll	32	32	shared memory	Y	0.0058	0.0017	61.5416	61.5491	-
semi	16	16	registers	N	0.0059	0.0061	95.2694	95.2814	72.0080
semi	16	16	shared memory	N	0.0058	0.0064	85.5186	85.5308	-
semi	16	16	registers	Y	0.0058	0.0062	97.1829	97.1949	71.4977
semi	16	16	shared memory	Y	0.0058	0.0073	84.4001	84.4131	-
semi	32	16	registers	N	0.0058	0.0059	78.8615	78.8732	58.5988
semi	32	16	shared memory	N	0.0058	0.0064	68.2108	68.2230	-
semi	32	16	registers	Y	0.0059	0.0063	74.5790	74.5913	60.6778
semi	32	16	shared memory	Y	0.0058	0.0074	67.2830	67.2962	-
semi	32	32	registers	N	0.0058	0.0059	77.1509	77.1625	57.3438
semi	32	32	shared memory	N	0.0057	0.0064	67.5627	67.5748	-
semi	32	32	registers	Y	0.0058	0.0060	75.6306	75.6424	60.0624
semi	32	32	shared memory	Y	0.0058	0.0071	62.1689	62.1818	-

Table 18. Time measurements for 2.5D templates on MI210.

Configurations				StencilPy				Manual Code
Template	Dx	Dy	Dz	Frontend	Code Gen	Kernel	Time to Solution	Time to Solution
gmem	8	8	8	0.0030	0.0022	24.5146	24.5198	53.3380
gmem	16	8	8	0.0030	0.0021	22.0717	22.0768	54.4676
gmem	32	4	4	0.0031	0.0022	22.9124	22.9177	50.3984
gmem	32	8	4	0.0031	0.0020	23.2463	23.2513	54.8803
gmem	64	4	4	0.0030	0.0019	23.2681	23.2731	56.4511
f4	8	8	8	0.0031	0.0025	24.5090	24.5146	-
f4	16	8	8	0.0029	0.0026	21.5094	21.5149	-
f4	32	4	4	0.0031	0.0025	21.8574	21.8629	-
f4	32	8	4	0.0030	0.0024	22.7870	22.7923	-
f4	64	4	4	0.0031	0.0027	22.5705	22.5763	-
smem	8	8	8	0.0031	0.0027	85.9694	85.9752	93.8043
smem	16	8	8	0.0030	0.0025	75.0853	75.0908	84.5964
smem	32	4	4	0.0030	0.0025	82.1255	82.1310	84.0707
smem	32	8	4	0.0030	0.0025	62.9853	62.9908	74.2236
smem	64	4	4	0.0030	0.0026	75.6956	75.7011	79.1279

Table 19. Time measurements for 3D templates on Max 1100.

13.3 Developer Productivity

We evaluate developer productivity by comparing the effort required to achieve similar levels of performance. Table 23 shows the number of lines of code for implementing the same Acoustic ISO kernel using StencilPy and manual implementations. StencilPy-based implementations can massively improve developer productivity with significantly less code to write. The code is written in a logically global view, and developers do not need to know details about target architectures. For performance tuning, developers can parameterize the framework by selecting configurations without changing the source code.

StencilPy also improves developer productivity with a platform-agnostic DSL that can be easily ported to different hardware by reusing the same DSL code and switching to another backend. StencilPy’s modular design makes it straightforward to change the backend.

Because our DSL is embedded in Python, developers who already know Python should feel comfortable getting started. Even for newcomers to Python, learning Python is very straightforward, especially for developers with a background in another HPC language, such as C, C++, or Fortran.

Configurations					StencilPy				Manual Code
Template	Dx	Dy	Mem Type	Prefetching	Frontend	Code Gen	Kernel	Time to Solution	Time to Solution
shift	32	16	registers	N	0.0030	0.0029	133.7393	133.7452	242.3428
shift	32	16	shared memory	N	0.0030	0.0028	98.9958	99.0016	-
shift	32	16	registers	Y	0.0031	0.0075	129.7240	129.7346	-
shift	32	16	shared memory	Y	0.0029	0.0023	107.1414	107.1466	-
shift	32	32	registers	N	0.0030	0.0029	92.6146	92.6206	167.6336
shift	32	32	shared memory	N	0.0030	0.0025	114.7496	114.7551	-
shift	32	32	registers	Y	0.0030	0.0027	101.4717	101.4775	-
shift	32	32	shared memory	Y	0.0030	0.0024	94.2460	94.2515	-
shift	64	16	registers	N	0.0030	0.0029	103.8370	103.8429	175.3473
shift	64	16	shared memory	N	0.0031	0.0028	145.5384	145.5443	-
shift	64	16	registers	Y	0.0031	0.0028	113.4298	113.4357	-
shift	64	16	shared memory	Y	0.0031	0.0028	92.1443	92.1502	-
unroll	32	16	registers	N	0.0030	0.0104	192.7422	192.7556	242.6466
unroll	32	16	shared memory	N	0.0030	0.0025	98.9296	98.9351	-
unroll	32	16	registers	Y	0.0031	0.0109	149.5442	149.5581	-
unroll	32	16	shared memory	Y	0.0030	0.0028	107.0851	107.0909	-
unroll	32	32	registers	N	0.0030	0.0106	122.0667	122.0804	183.7820
unroll	32	32	shared memory	N	0.0030	0.0026	114.1484	114.1540	-
unroll	32	32	registers	Y	0.0030	0.0115	125.9463	125.9608	-
unroll	32	32	shared memory	Y	0.0030	0.0028	93.9452	93.9511	-
unroll	64	16	registers	N	0.0030	0.0109	132.4960	132.5100	195.3340
unroll	64	16	shared memory	N	0.0031	0.0028	145.5521	145.5580	-
unroll	64	16	registers	Y	0.0030	0.0111	140.8163	140.8303	-
unroll	64	16	shared memory	Y	0.0030	0.0025	92.2572	92.2627	-
semi	32	16	registers	N	0.0030	0.0096	186.5270	186.5396	229.6691
semi	32	16	shared memory	N	0.0030	0.0099	187.9715	187.9844	-
semi	32	16	registers	Y	0.0030	0.0092	146.9608	146.9729	-
semi	32	16	shared memory	Y	0.0029	0.0112	132.5459	132.5600	-
semi	32	32	registers	N	0.0029	0.0099	114.3396	114.3524	168.4991
semi	32	32	shared memory	N	0.0042	0.0141	112.7931	112.8114	-
semi	32	32	registers	Y	0.0030	0.0101	121.5178	121.5309	-
semi	32	32	shared memory	Y	0.0030	0.0112	106.9560	106.9702	-
semi	64	16	registers	N	0.0030	0.0092	127.8218	127.8340	185.7686
semi	64	16	shared memory	N	0.0078	0.0100	148.4514	148.4691	-
semi	64	16	registers	Y	0.0030	0.0097	138.0790	138.0917	-
semi	64	16	shared memory	Y	0.0029	0.0123	124.1082	124.1234	-

Table 20. Time measurements for 2.5D templates on Max 1100.

Template	Dx	Dy	Dz	Grid	Frontend	Code Gen	Kernel	Time to Solution
cube	19	19	19	19	0.0025	0.0008	170.1158	172.0198
plane	19	19	19	19	0.0026	0.0008	125.4266	127.2942
semi	19	19	19	19	0.0034	0.0010	146.2562	148.1321
cube	19	19	19	29	0.0025	0.0021	264.2300	266.3075
plane	58	58	60	60	0.0025	0.0013	3,767.2723	3,769.2409
semi	57	57	60	60	0.0027	0.0021	4,316.1766	4,318.1728

Table 21. Time measurements on STX Simulator.

Backend	Template	Device	Frontend	Code Gen	Kernel	Time to Solution	Manual Code
OMP	loop	Genoa	0.0033	0.0011	269.4177	269.4222	274.6220
CUDA	f4	H100	0.0048	0.0024	45.0160	45.0232	45.7835
HIP	gmem	MI210	0.0059	0.0012	138.1122	138.1193	150.5630
CSL	csl	CS2	0.0034	0.0011	0.4685	0.4730	0.4676

Table 22. Time measurements for CSL backend and comparisons with other selected backends.

14 SUMMARY

We presented StencilPy, a portable framework for accelerating high-order stencils on modern CPUs, GPUs, and emerging architectures. While still under active development, it already demonstrates promising results: it generates code for a variety of platforms with great performance, demonstrates strong performance portability spanning various hardware vendors and generations, and enhances developer productivity with a user-friendly domain-specific language.

This manuscript describes the StencilPy framework, including its multi-layered architectural design, code analysis, code generation, and execution. It discusses the workflow of the framework and the template engine that powers the multiple backends. It evaluates the framework from the perspectives of numerical correctness, runtime performance, performance portability, and developer productivity. It demonstrates the approaches that can be used to accelerate high-order stencils to facilitate development, ease experiments, and reduce overheads.

15 FUTURE WORK

Here, we sketch possible extensions to this work.

15.1 Optimizations to StencilPy’s Generated Code

Our work continues the performance tuning effort to further optimize the runtime performance of the generated code. Specifically, for GPU backends, our roadmap includes optimizations such as consolidating conditional checks to

StencilPy	Template	Prefetching	CUDA/HIP	SYCL
285	gmem	-	1115	1105
	f4	-	1145	-
	smem	-	1215	1160
	shift	N	1208	1268
	shift	Y	1427	
	unroll	N	1191	1253
	unroll	Y	1419	
	semi	N	1247	1269
	semi	Y	1480	
	Template	OMP	Template	STX
	loop	655	cube	1034
	loop_blocking	713	plane	1080
	loop_blocking_collapse	703	semi	1116
	taskloop	696	Template	CSL
task_blocking	675	cs2	1977	

Table 23. Lines of code for implementing Acoustic ISO using StencilPy v.s. manually crafted code.

minimize branch divergence and using pinned memory to accelerate data transfers between the host and GPU devices. Additionally, we aim to optimize register allocations to alleviate register pressure and improve occupancy.

In the case of the SYCL programming model, where loop unrolling is not recommended, we propose generating code using a regular for loop for the 2.5D streaming approach and evaluating the performance impacts.

For the CSL backend, we plan to introduce support for PE dimension divisions to handle larger data grids on a CS-2. In addition, we aim to reduce the footprint by carefully allocating colors and local task identifiers from a limited quota while preserving the asynchronous memory copy feature. Our proposed approach involves shifting more logic from callback tasks to state machine transitions.

Furthermore, our plans include implementing other enhancements tailored to the specifics of the programming model.

15.2 Auto-Tuning StencilPy

The StencilPy framework we presented in this article uses a user-guided approach, and we plan to incorporate auto-tuning capabilities. Auto-tuning involves generating multiple code versions and dynamically selecting tuning parameters based on runtime properties and stencil characteristics. To facilitate this, we need to define a cost model for selecting kernel candidates and introduce a feedback mechanism that allows dynamic code version switching during runtime to alternative candidates if the currently selected one fails to meet performance expectations during execution.

In addition, this capability will empower StencilPy to switch among templates and optimization strategies during runtime dynamically. As the computation progresses, the data utilized in the computation may change, such as transitioning from sparse to dense or centering around specific perturbation points before evening out. This dynamic

adaptation allows the computation to efficiently utilize different templates and optimizations as the iteration unfolds, optimizing performance for long-duration executions with evolving data patterns. The built-in profiler and the Just-In-Time compilation in our framework serve as technical foundations of this extended work. Our optimized code generation and compilation require little time, making the overhead from dynamic switching negligible, especially for long-duration execution.

Furthermore, to enhance the accuracy and speed of auto-tuning, we anticipate exploring the incorporation of machine-learning techniques into the framework. This addition further refines and speeds up the auto-tuning process, ensuring optimal performance across varying stencil applications and data patterns.

15.3 StencilPy Frontend Extensions

We plan to introduce one additional user-facing frontend interface on top of the current domain-specific language, enabling domain application developers to express stencil computations at a higher-level abstraction. Aiming to cater to a broader user base, including geoscientists and physicists, this extension is intended to express math and physics formulas for scientific simulations that essentially use stencil computations.

15.4 StencilPy Backend Extensions

We plan to incorporate FPGAs as a special backend in StencilPy. StencilPy already can generate SYCL code, which inherently supports FPGAs. Our next step will involve evaluating the performance of StencilPy-generated code on FPGA devices using generated SYCL code. If the outcomes prove promising, we can consider the development of a dedicated backend tailored specifically for FPGA devices.

Furthermore, we plan to explore the feasibility of using MLIR [34] as a virtual backend and evaluate its performance benefits. While StencilPy already supports a variety of architectures, the motivation for MLIR integration is to leverage its built-in optimization phases before generating device-specific binaries.

15.5 StencilPy Framework Distribution

We plan to explore Python's distribution model to facilitate support for diverse backends, including various host platforms and device machines. Additionally, we aim to open-source the tool, increasing accessibility, collecting feedback, and fostering collaboration within the community.

ACKNOWLEDGMENTS

This work was supported in part by a contract from TotalEnergies EP Research & Technology USA, LLC. We thank Timo Eichmann, François Hamon, Marc Andre Heller, Mathias Jacquelin, Jens Krüger, Jie Meng, Kai Plociennik, and Sameer Shende for their support of this work. We gratefully acknowledge the computing resources provided by Joint Laboratory for System Evaluation at Argonne National Laboratory, Oak Ridge Leadership Computing Facility, University of Oregon, Rice University, and TotalEnergies.

REFERENCES

- [1] M. Abadi, A. Agarwal, P. Barham, E. Brevdo, Z. Chen, C. Citro, G. S. Corrado, A. Davis, J. Dean, M. Devin, S. Ghemawat, I. Goodfellow, A. Harp, G. Irving, M. Isard, Y. Jia, R. Jozefowicz, L. Kaiser, M. Kudlur, J. Levenberg, D. Mané, R. Monga, S. Moore, D. Murray, C. Olah, M. Schuster, J. Shlens, B. Steiner, I. Sutskever, K. Talwar, P. Tucker, V. Vanhoucke, V. Vasudevan, F. Viégas, O. Vinyals, P. Warden, M. Wattenberg, M. Wicke, Y. Yu, and X. Zheng. TensorFlow: Large-Scale Machine Learning on Heterogeneous Systems, 2015. Software available from tensorflow.org.

- [2] O. Antepara, S. Williams, H. Johansen, T. Zhao, S. Hirsch, P. Goyal, and M. Hall. Performance Portability Evaluation of Blocked Stencil Computations on GPUs. In *Proceedings of the SC '23 Workshops of The International Conference on High Performance Computing, Networking, Storage, and Analysis*, SC-W '23, page 1007–1018, New York, NY, USA, 2023. Association for Computing Machinery.
- [3] R. Baghdadi, U. Beaugnon, A. Cohen, T. Grosser, M. Kruse, C. Reddy, S. Verdoolaege, A. Betts, A. F. Donaldson, J. Ketema, J. Absar, S. Van Haastregt, A. Kravets, A. Lokhmotov, R. David, and E. Hajjiev. PENCIL: A Platform-Neutral Compute Intermediate Language for Accelerator Programming. In *2015 International Conference on Parallel Architecture and Compilation (PACT)*, pages 138–149, Oct. 2015.
- [4] R. Baghdadi, J. Ray, M. B. Romdhane, E. Del Sozzo, A. Akkas, Y. Zhang, P. Suriana, S. Kamil, and S. Amarasinghe. Tiramisu: a polyhedral compiler for expressing fast and portable code. In *Proceedings of the 2019 IEEE/ACM International Symposium on Code Generation and Optimization*, CGO 2019, pages 193–205, Washington, DC, USA, Feb. 2019. IEEE Press.
- [5] V. Bandishti, I. Pananilath, and U. Bondhugula. Tiling stencil computations to maximize parallelism. In *SC '12: Proceedings of the International Conference on High Performance Computing, Networking, Storage and Analysis*, pages 1–11, Nov. 2012. ISSN: 2167-4337.
- [6] M. Bauer, J. Hötzer, D. Ernst, J. Hammer, M. Seiz, H. Hierl, J. Hönig, H. Köstler, G. Wellein, B. Nestler, and U. Rüde. Code Generation for Massively Parallel Phase-Field Simulations. In *Proceedings of the International Conference for High Performance Computing, Networking, Storage and Analysis*, SC '19, New York, NY, USA, 2019. Association for Computing Machinery.
- [7] U. Bondhugula, A. Hartono, J. Ramanujam, and P. Sadayappan. A practical automatic polyhedral parallelizer and locality optimizer. *ACM SIGPLAN Notices*, 43(6):101–113, June 2008.
- [8] Cerebras. Wafer-Scale Deep Learning. In *2019 IEEE Hot Chips 31 Symposium (HCS)*, pages 1–31, Los Alamitos, CA, USA, August 2019. IEEE Computer Society.
- [9] Cerebras. Cerebras SDK Documentation (1.0.0). URL: <https://sdk.cerebras.net/>, November 2023.
- [10] M. Christen, O. Schenk, and H. Burkhart. PATUS: A Code Generation and Autotuning Framework for Parallel Iterative Stencil Computations on Modern Microarchitectures. In *2011 IEEE International Parallel Distributed Processing Symposium*, pages 676–687, May 2011.
- [11] R. Cytron, A. Lowry, and F. K. Zadeck. Code Motion of Control Structures in High-Level Languages. In *Proceedings of the 13th ACM SIGACT-SIGPLAN Symposium on Principles of Programming Languages*, POPL '86, page 70–85, New York, NY, USA, 1986. Association for Computing Machinery.
- [12] R. de la Cruz and M. Araya-Polo. Algorithm 942: Semi-stencil. *ACM Transactions on Mathematical Software*, 40(3):23:1–23:39, Apr. 2014.
- [13] R. de la Cruz, M. Araya-Polo, and J. M. Cela. Introducing the Semi-stencil Algorithm. In R. Wyrzykowski, J. Dongarra, K. Karczewski, and J. Wasniewski, editors, *Parallel Processing and Applied Mathematics*, Lecture Notes in Computer Science, pages 496–506, Berlin, Heidelberg, 2010. Springer.
- [14] European Processor Initiative. Domain specific accelerators in EPI STX (stencil/tensor accelerator). URL: <https://www.european-processor-initiative.eu/wp-content/uploads/2019/12/EPI-Technology-FS-STX.pdf>, December 2019.
- [15] M. Frigo, C. E. Leiserson, H. Prokop, and S. Ramachandran. Cache-Oblivious Algorithms. In *Proceedings of the 40th Annual Symposium on Foundations of Computer Science*, FOCS '99, page 285, USA, Oct. 1999. IEEE Computer Society.
- [16] M. Frigo and V. Strumpen. Cache oblivious stencil computations. In *Proceedings of the 19th annual international conference on Supercomputing*, ICS '05, pages 361–366, Cambridge, Massachusetts, June 2005. Association for Computing Machinery.
- [17] M. Frigo and V. Strumpen. The cache complexity of multithreaded cache oblivious algorithms. In *Proceedings of the eighteenth annual ACM symposium on Parallelism in algorithms and architectures*, SPAA '06, pages 271–280, Cambridge, Massachusetts, USA, July 2006. Association for Computing Machinery.
- [18] O. Fuhrer, C. Osuna, X. Lapillonne, T. Gysi, B. Cumming, M. Bianco, A. Arteaga, and T. Schulthess. Towards a performance portable, architecture agnostic implementation strategy for weather and climate models. *Supercomputing Frontiers and Innovations: an International Journal*, 1(1):45–62, Apr. 2014.
- [19] Fujitsu. Fujitsu High Performance CPU for the Post-K Computer. URL: <https://www.fujitsu.com/global/documents/solutions/business-technology/tc/catalog/20180821hotchips30.pdf>, August 2018.
- [20] J.-M. Gorius and T. Grosser. Modeling Stencils in a Multi-Level Intermediate Representation. URL: https://jmgorius.com/pdf/ENS_Rennes_DIT_M1_2019_paper.pdf, 2019.
- [21] T. Grosser, A. Cohen, P. H. J. Kelly, J. Ramanujam, P. Sadayappan, and S. Verdoolaege. Split tiling for GPUs: automatic parallelization using trapezoidal tiles. In *Proceedings of the 6th Workshop on General Purpose Processor Using Graphics Processing Units*, pages 24–31, Houston, Texas, USA, Mar. 2013. Association for Computing Machinery.
- [22] T. Gysi, C. Müller, O. Zinenko, S. Herhut, E. Davis, T. Wicky, O. Fuhrer, T. Hoefler, and T. Grosser. Domain-Specific Multi-Level IR Rewriting for GPU: The Open Earth Compiler for GPU-accelerated Climate Simulation. *ACM Trans. Archit. Code Optim.*, 18(4), September 2021.
- [23] T. Gysi, C. Osuna, O. Fuhrer, M. Bianco, and T. C. Schulthess. STELLA: a domain-specific tool for structured grid methods in weather and climate models. In *SC '15: Proceedings of the International Conference for High Performance Computing, Networking, Storage and Analysis*, pages 1–12, 2015.
- [24] C. R. Harris, K. J. Millman, S. J. van der Walt, R. Gommers, P. Virtanen, D. Cournapeau, E. Wieser, J. Taylor, S. Berg, N. J. Smith, R. Kern, M. Picus, S. Hoyer, M. H. van Kerkwijk, M. Brett, A. Haldane, J. F. del Río, M. Wiebe, P. Peterson, P. Gérard-Marchant, K. Sheppard, T. Reddy, W. Weckesser, H. Abbasi, C. Gohlke, and T. E. Oliphant. Array programming with NumPy. *Nature*, 585(7825):357–362, Sept. 2020.
- [25] J. Holewinski, L.-N. Pouchet, and P. Sadayappan. High-performance code generation for stencil computations on GPU architectures. In *Proceedings of the 26th ACM international conference on Supercomputing*, ICS '12, pages 311–320, San Servolo Island, Venice, Italy, June 2012. Association for Computing Machinery.

- [26] Y. Hu. The Taichi Programming Language. In *ACM SIGGRAPH 2020 Courses*, SIGGRAPH '20, New York, NY, USA, 2020. Association for Computing Machinery.
- [27] Intel. oneAPI GPU Optimization Guide. URL: https://cdrdv2-public.intel.com/773648/oneapi_optimization_guide-gpu_2023.1-771772-773648.pdf, December 2023.
- [28] M. Jacquelin, M. Araya-Polo, and J. Meng. Scalable Distributed High-Order Stencil Computations. In *Proceedings of the International Conference on High Performance Computing, Networking, Storage and Analysis*, SC '22. IEEE Press, 2022.
- [29] G. Jin, J. Mellor-Crummey, and R. Fowler. Increasing temporal locality with skewing and recursive blocking. In *Proceedings of the 2001 ACM/IEEE conference on Supercomputing*, SC '01, page 43, Denver, Colorado, Nov. 2001. Association for Computing Machinery.
- [30] D. Komatitsch and J. Tromp. A perfectly matched layer absorbing boundary condition for the second-order seismic wave equation. *Geophysical Journal International*, 154(1):146–153, July 2003.
- [31] S. Krishnamoorthy, M. Baskaran, U. Bondhugula, J. Ramanujam, A. Rountev, and P. Sadayappan. Effective automatic parallelization of stencil computations. *ACM SIGPLAN Notices*, 42(6):235–244, June 2007.
- [32] S. K. Lam, A. Pitrou, and S. Seibert. Numba: A llvm-based python jit compiler. In *Proceedings of the Second Workshop on the LLVM Compiler Infrastructure in HPC*, pages 1–6, 2015.
- [33] C. Lattner and V. Adve. LLVM: A Compilation Framework for Lifelong Program Analysis and Transformation. pages 75–88, San Jose, CA, USA, Mar. 2004.
- [34] C. Lattner, M. Amini, U. Bondhugula, A. Cohen, A. Davis, J. Pienaar, R. Riddle, T. Shpeisman, N. Vasilache, and O. Zinenko. MLIR: A Compiler Infrastructure for the End of Moore’s Law. *arXiv:2002.11054 [cs]*, Feb. 2020. arXiv: 2002.11054.
- [35] M. Louboutin, M. Lange, F. Luporini, N. Kukreja, P. A. Witte, F. J. Herrmann, P. Velesko, and G. J. Gorman. Devito (v3.1.0): an embedded domain-specific language for finite differences and geophysical exploration. *Geoscientific Model Development*, 12(3):1165–1187, Mar. 2019. Publisher: Copernicus GmbH.
- [36] F. Luporini, M. Louboutin, M. Lange, N. Kukreja, P. Witte, J. Hückelheim, C. Yount, P. H. J. Kelly, F. J. Herrmann, and G. J. Gorman. Architecture and Performance of Devito, a System for Automated Stencil Computation. *ACM Transactions on Mathematical Software*, 46(1):6:1–6:28, April 2020.
- [37] M. Lücke, M. Steuwer, and A. Smith. A functional pattern-based language in MLIR. URL: <https://michel.steuwer.info/files/publications/2020/accML.pdf>, 2020.
- [38] K. Matsumura, H. R. Zohouri, M. Wahib, T. Endo, and S. Matsuoka. Artifact to manifest paper “AN5D: automated stencil framework for high-degree temporal blocking on GPUs”. URL: <https://github.com/khaki3/AN5D-Artifact>, December 2019.
- [39] K. Matsumura, H. R. Zohouri, M. Wahib, T. Endo, and S. Matsuoka. AN5D: automated stencil framework for high-degree temporal blocking on GPUs. In *Proceedings of the 18th ACM/IEEE International Symposium on Code Generation and Optimization*, pages 199–211, San Diego, CA, USA, Feb. 2020. Association for Computing Machinery.
- [40] J. McCalpin and D. Wonnacott. Time Skewing: A Value-Based Approach to Optimizing for Memory Locality. URL: <https://scholarship.libraries.rutgers.edu/esploro/outputs/technicalDocumentation/Time-Skewing-A-Value-Based-Approach-to/991031549998604646>, 1998.
- [41] J. Meng, A. Atle, H. Calandra, and M. Araya-Polo. Minimod: A Finite Difference solver for Seismic Modeling. *arXiv:2007.06048v1*, July 2020.
- [42] P. Micikevicius. 3D finite difference computation on GPUs using CUDA. In *Proceedings of 2nd Workshop on General Purpose Processing on Graphics Processing Units, GPGPU-2*, pages 79–84, Washington, D.C., USA, Mar. 2009. Association for Computing Machinery.
- [43] Modular. *Mojo Manual*, Mar. 2024. Available at <https://docs.modular.com/mojo/manual/>.
- [44] A. Nguyen, N. Satish, J. Chhugani, C. Kim, and P. Dubey. 3.5-D Blocking Optimization for Stencil Computations on Modern CPUs and GPUs. In *SC '10: Proceedings of the 2010 ACM/IEEE International Conference for High Performance Computing, Networking, Storage and Analysis*, pages 1–13, Nov. 2010. ISSN: 2167-4337.
- [45] A. Paszke, S. Gross, F. Massa, A. Lerer, J. Bradbury, G. Chanan, T. Killeen, Z. Lin, N. Gimelshein, L. Antiga, A. Desmaison, A. Köpf, E. Yang, Z. DeVito, M. Raison, A. Tejani, S. Chilamkurthy, B. Steiner, L. Fang, J. Bai, and S. Chintala. *PyTorch: An Imperative Style, High-Performance Deep Learning Library*. Curran Associates Inc., Red Hook, NY, USA, 2019.
- [46] J. Ragan-Kelley, C. Barnes, A. Adams, S. Paris, F. Durand, and S. Amarasinghe. Halide: a language and compiler for optimizing parallelism, locality, and recomputation in image processing pipelines. In *Proceedings of the 34th ACM SIGPLAN Conference on Programming Language Design and Implementation*, PLDI '13, pages 519–530, Seattle, Washington, USA, June 2013. Association for Computing Machinery.
- [47] E. Raut, J. Meng, M. Araya-Polo, and B. Chapman. Evaluating Performance of OpenMP Tasks in a Seismic Stencil Application. In K. Milfeld, B. R. de Supinski, L. Koesterke, and J. Klinkenberg, editors, *OpenMP: Portable Multi-Level Parallelism on Modern Systems*, pages 67–81, Cham, 2020. Springer International Publishing.
- [48] P. Rawat, M. Kong, T. Henretty, J. Holewinski, K. Stock, L.-N. Pouchet, J. Ramanujam, A. Rountev, and P. Sadayappan. SDSLc: a multi-target domain-specific compiler for stencil computations. In *Proceedings of the 5th International Workshop on Domain-Specific Languages and High-Level Frameworks for High Performance Computing*, WOLFHPC '15, pages 1–10, Austin, Texas, Nov. 2015. Association for Computing Machinery.
- [49] P. S. Rawat, F. Rastello, A. Sukumaran-Rajam, L.-N. Pouchet, A. Rountev, and P. Sadayappan. Register optimizations for stencils on GPUs. *ACM SIGPLAN Notices*, 53(1):168–182, Feb. 2018.
- [50] P. S. Rawat, M. Vaidya, A. Sukumaran-Rajam, M. Ravishanker, V. Grover, A. Rountev, L.-N. Pouchet, and P. Sadayappan. Domain-Specific Optimization and Generation of High-Performance GPU Code for Stencil Computations. *Proceedings of the IEEE*, 106(11):1902–1920, Nov. 2018. Conference Name: Proceedings of the IEEE.

- [51] P. S. Rawat, M. Vaidya, A. Sukumaran-Rajam, A. Rountev, L.-N. Pouchet, and P. Sadayappan. On Optimizing Complex Stencils on GPUs. In *2019 IEEE International Parallel and Distributed Processing Symposium (IPDPS)*, pages 641–652, May 2019. ISSN: 1530-2075.
- [52] K. Rocki, D. Van Essendelft, I. Sharapov, R. Schreiber, M. Morrison, V. Kibardin, A. Portnoy, J. F. Dietiker, M. Syamlal, and M. James. Fast Stencil-Code Computation on a Wafer-Scale Processor. In *Proceedings of the International Conference for High Performance Computing, Networking, Storage and Analysis, SC '20*. IEEE Press, 2020.
- [53] G. Roth, S. Carr, J. Mellor-Crummey, and K. Kennedy. A General Stencil Compilation Strategy for Distributed-Memory Machines. URL: <https://softlib.rice.edu/pub/CRPC-TRs/reports/CRPC-TR96652-S.pdf>, July 2001.
- [54] G. Roth, J. Mellor-Crummey, K. Kennedy, and R. G. Brickner. Compiling stencils in high performance Fortran. In *Proceedings of the 1997 ACM/IEEE Conference on Supercomputing, SC '97*, page 1–20, New York, NY, USA, 1997. Association for Computing Machinery.
- [55] R. Sai, M. Jacquelin, F. P. Hamon, M. Araya-Polo, and R. R. Settgast. Massively Distributed Finite-Volume Flux Computation. In *ScalAH23: 14th Workshop on Latest Advances in Scalable Algorithms for Large-Scale Heterogeneous Systems*, 2023.
- [56] R. Sai, J. Mellor-Crummey, M. A. Heller, J. Kruger, and M. Araya-Polo. Wave Propagation on the STX Accelerator. In *Rice EnergyHPC Conference 2023, Houston, TX, 2023*.
- [57] R. Sai, J. Mellor-Crummey, X. Meng, M. Araya-Polo, and J. Meng. Accelerating High-Order Stencils on GPUs. In *2020 IEEE/ACM Performance Modeling, Benchmarking and Simulation of High Performance Computer Systems (PMBS)*, pages 86–108, 2020.
- [58] R. Sai, J. Mellor-Crummey, X. Meng, M. Araya-Polo, and J. Meng. Using the Semi-Stencil Algorithm to Accelerate High-Order Stencils on GPUs. In *2021 International Workshop on Performance Modeling, Benchmarking and Simulation of High Performance Computer Systems (PMBS)*, pages 63–68, 2021.
- [59] R. Sai, J. Mellor-Crummey, X. Meng, K. Zhou, M. Araya-Polo, and J. Meng. Accelerating high-order stencils on GPUs. *Concurrency and Computation: Practice and Experience*, 34(20):e6467, 2022.
- [60] Y. Song and Z. Li. New tiling techniques to improve cache temporal locality. In *Proceedings of the ACM SIGPLAN 1999 conference on Programming language design and implementation*, pages 215–228, Atlanta, Georgia, USA, May 1999. Association for Computing Machinery.
- [61] M. Steuwer, T. Rimmelg, and C. Dubach. LIFT: A functional data-parallel IR for high-performance GPU code generation. In *2017 IEEE/ACM International Symposium on Code Generation and Optimization (CGO)*, pages 74–85, Feb. 2017.
- [62] R. Strzodka, M. Shaheen, D. Pajak, and H.-P. Seidel. Cache oblivious parallelograms in iterative stencil computations. In *Proceedings of the 24th ACM International Conference on Supercomputing, Tsukuba, Ibaraki, Japan, June 2010*. Association for Computing Machinery.
- [63] Y. Tang, R. A. Chowdhury, B. C. Kuszmaul, C.-K. Luk, and C. E. Leiserson. The Pochoir Stencil Compiler. In *Proceedings of the twenty-third annual ACM symposium on Parallelism in algorithms and architectures, SPAA'11*, pages 117–128, San Jose, California, USA, June 2011. Association for Computing Machinery.
- [64] D. Wonnacott. Using time skewing to eliminate idle time due to memory bandwidth and network limitations. In *Proceedings 14th International Parallel and Distributed Processing Symposium. IPDPS 2000*, pages 171–180, May 2000.
- [65] D. Wonnacott. Achieving Scalable Locality with Time Skewing. *International Journal of Parallel Programming*, 30(3):181–221, June 2002.
- [66] T. Zhou, J. Shirako, and V. Sarkar. APPy: Annotated Parallelism for Python on GPUs. In *Proceedings of the 33rd ACM SIGPLAN International Conference on Compiler Construction, CC 2024*, page 113–125, New York, NY, USA, 2024. Association for Computing Machinery.